

Gravitational Waves in Brans-Dicke Theory : Analysis by Test Particles around a Kerr Black Hole

MOTOYUKI SAIJO[†], HISA-AKI SHINKAI[‡] and KEI-ICHI MAEDA[§]

Department of Physics, Waseda University, Shinjuku-ku, Tokyo 169, Japan ^{†,§}
and
Department of Physics, Washington University, St. Louis, MO63130-4899, USA [‡]

Abstract

Analyzing test particles falling into a Kerr black hole, we study gravitational waves in Brans-Dicke theory of gravity. First we consider a test particle plunging with a constant azimuthal angle into a rotating black hole and calculate the waveform and emitted energy of both scalar and tensor modes of gravitational radiation. We find that the waveform as well as the energy of the scalar gravitational waves weakly depends on the rotation parameter of black hole a and on the azimuthal angle.

Secondly, using a model of a non-spherical dust shell of test particles falling into a Kerr black hole, we study when the scalar modes dominate. When a black hole is rotating, the tensor modes do not vanish even for a “spherically symmetric” shell, instead a slightly oblate shell minimizes their energy but with non-zero finite value, which depends on Kerr parameter a . As a result, we find that the scalar modes dominate only for highly spherical collapse, but they never exceed the tensor modes unless the Brans-Dicke parameter $\omega_{BD} \lesssim 750$ for $a/M = 0.99$ or unless $\omega_{BD} \lesssim 20,000$ for $a/M = 0.5$, where M is mass of black hole.

We conclude that the scalar gravitational waves with $\omega_{BD} \lesssim$ several thousands do not dominate except for very limited situations (observation from the face-on direction of a test particle falling into a Schwarzschild black hole or highly spherical dust shell collapse into a Kerr black hole). Therefore observation of polarization is also required when we determine the theory of gravity by the observation of gravitational waves.

December, 1996

[†] Electronic mail : 696L0482@mn.waseda.ac.jp
[‡] Electronic mail : shinkai@wurel.wustl.edu
[§] Electronic mail : maeda@mn.waseda.ac.jp

I. INTRODUCTION

After the discovery of the binary pulsar PSR1916+13 by Hulse and Taylor [1], we believe in the existence of gravitational waves emitted from compact objects. Their continual observations over 20 years show that both the observed change rate of the orbital period and that predicted by general relativity agree to within 0.3% accuracy [2].

Currently, a number of worldwide projects for detecting gravitational radiation directly using a km-scale laser interferometer such as LIGO, VIRGO, GEO600, and TAMA are progressing. In particular, the LIGO project [3] will begin operating within a few years. Among the many possible sources of gravitational waves, one expected plausible source is a coalescing binary, composed of neutron star-neutron star (NS-NS), neutron star-black hole (NS-BH), or black hole-black hole (BH-BH). These direct detections of gravitational waves will enable us to see strong gravitational phenomena such as coalescence of compact stars or black holes. In order to extract signals from noise, we need to prepare in advance a list of expected templates of gravitational waves, which depend on many parameters of sources (masses and spins of compact objects, orbital angular momentum, eccentricity of their orbits, \dots). Therefore one of the current most important subjects in general relativity is to predict a precise waveform of gravitational waves for a set of given parameters.

Furthermore, if we can directly observe gravitational waves, we may also put some constraints on the theories of gravity, or we might find some evidence for alternative theories of gravity instead of general relativity. Although many alternatives have been proposed, most of them have been rejected by experiments or observations except for a few theories such as scalar tensor theories of gravity. As the simplest and proto-type among all scalar-tensor theories of gravity, the Brans-Dicke (BD) theory [4] of gravity is often considered as an alternative. We know the strictest bound for BD theory is to the BD parameter $\omega_{BD} \gtrsim 500$ (the infinity limit of ω_{BD} is just general relativity), which was made by the observation of the Shapiro time delay using Viking on Mars [5]. The possibilities of testing gravity theory using gravitational radiation as a tool were also considered in the early days [6,7], but it was not effective in the weak gravitational field of the solar-system.

Using the binary pulsar PSR1913+16, the consistency of general relativity was tested, as we mentioned above. This binary was also considered as a tool for checking other gravity theories [8,9]. Recent analysis by Will and Zaglauer [10], however, concluded that this source cannot be used for testing BD theory effectively. This is because the two neutron stars in the binary are believed to have nearly equal masses, and the limit is also sensitive to the star models, hence the restriction on ω_{BD} was weak. These classical tests, however, are carried out only in the weak gravitational field. On the contrary, observing gravitational waves directly from compact sources such as a BH-BH system will clarify some phenomena in strong gravitational fields and may determine which theory of gravity is correct. In order to analyze it from observational data, we also have to prepare a list of templates of waveforms for other theories of gravity. In BD theory, gravitational waves have three modes, i.e., a scalar mode, which we call a scalar gravitational wave (SGW), as well as two tensor modes (+ and \times modes) of conventional gravitational waves, which we shall call tensor gravitational waves (TGWs) here. Will [11] studied a constrained bound of ω_{BD} from observing the inspiralling phase of compact binaries, and concluded that a bound strongly depends on mass difference between components. To find the expected templates of SGWs,

Shibata, Nakao and Nakamura (SNN) [12] calculated the waveform of SGWs from spherically symmetrical dust fluid collapse and concluded that the advanced LIGO may detect SGWs even if the BD coupling constant ω_{BD} is $10^4 \sim 10^6$.

In this paper, we extend SNN's studies and figure out more aspects of both SGWs and TGWs behavior in BD theory. Since a spherical symmetrical system is just an idealized model, if we consider a more realistic situation such as the case that spherical symmetry is no longer valid, we may wonder whether SGWs can be really detected alongside TGW contributions. If we can observe the signals with the full polarization information of gravitational waves, then we can extract the scalar modes and do not need to worry about whether the TGWs will dominate the SGWs. However, if we have few observational bases, we may not be able to separate the polarizations. Hence it may be important to clarify in which situation the SGWs can dominate. Therefore, we study gravitational waves in BD theory and compare those scalar and tensor modes, analyzing test particle motions around a rotating black hole. We analyze two cases: First, we calculate the waveforms and emitted energy both of SGWs and of TGWs by a test particle plunging with a constant azimuthal angle into a rotating black hole. This linearized analysis using a test particle is known to have a reasonably good agreement with fully relativistic numerical simulations in some cases such as a head-on collision of two black holes [13]. Our case, we believe, also mimics a collision of two compact objects in BD theory.

As for gravitational waves from gravitational collapse such as a supernova explosion followed by a formation of a neutron star, we know that no tensor modes are generated in a spherically symmetric case. Although the SGWs are still emitted in such a case and the theory of gravity might be determined by observing such SGWs, an ansatz of spherical symmetry is extremely idealized. Therefore, we next analyze a non-spherical dust shell collapsing into a rotating black hole. Comparing the SGWs and TGWs, we can see how much deviation from spherical symmetry still gives us the domination of the SGWs. We then discuss the possibility of identification of the SGWs without observing polarization.

This paper is organized as follows. In §2, we present our basic equations for calculating gravitational radiation in BD theory. We then analyze the waveforms and energy both of the tensor and of the scalar modes by a test particle plunging into a rotating black hole in §3. We also analyze non-spherically symmetric dust-shell collapse onto a Kerr black hole in §4. §5 is devoted to our conclusions and some remarks. Throughout this paper, we use the units of $c = G_N = 1$ [14] and the notations and definitions such as Christoffel symbols and curvature follow Misner-Thorne-Wheeler [15].

II. BRANS-DICKE THEORY AND BLACK HOLE PERTURBATIONS

BD theory [4] is the simplest version of scalar-tensor theories of gravity in which a scalar field couples with metric tensor fields. The action S of BD theory is given by

$$S = \int d^4x \sqrt{-g} \left[\frac{1}{16\pi} \left(\phi R - \frac{\omega_{BD}}{\phi} g^{\mu\nu} \nabla_\mu \phi \nabla_\nu \phi \right) \right] + S_{matter}, \quad (1)$$

where the coupling constant ω_{BD} is called the BD parameter. The theory is reduced to general relativity in the limit of $\omega_{BD} \rightarrow \infty$. The conservative observational bound on ω_{BD}

is $\omega_{BD} > 500$, which is obtained from the Shapiro time delay experiment [16].

From the action (1), the field equations become

$$G_{\mu\nu} = \frac{8\pi}{\phi} T_{\mu\nu} + \frac{\omega_{BD}}{\phi^2} \left[(\nabla_\mu \phi)(\nabla_\nu \phi) - \frac{1}{2} g_{\mu\nu} (\nabla \phi)^2 \right] + \frac{1}{\phi} (\nabla_\mu \nabla_\nu \phi - g_{\mu\nu} \square \phi), \quad (2)$$

$$\square \phi = \frac{8\pi}{3 + 2\omega_{BD}} T, \quad (3)$$

where $G_{\mu\nu} = R_{\mu\nu} - \frac{1}{2} g_{\mu\nu} R$ is the Einstein tensor. Before we discuss perturbations of a black hole spacetime, it may be more convenient to introduce the Einstein frame, in which the metric and scalar perturbations are decoupled. Using the conformal transformation from the physical (Jordan-Brans-Dicke) frame to the Einstein frame as

$$g_{\mu\nu}^{(E)} = \left(\frac{\phi}{\phi_0} \right) g_{\mu\nu}, \quad (4)$$

the basic equations (2) and (3) are written as

$$G_{\mu\nu}^{(E)} = 8\pi (T_{\mu\nu}^{(E)} + T_{\mu\nu}^{(\Phi)}) \quad (5)$$

$$\square^{(E)} \Phi = 2 \left(\frac{\pi}{3 + 2\omega_{BD}} \right)^{1/2} T^{(E)}, \quad (6)$$

where ϕ_0 is a constant, which is fixed by our ansatz $G_N = 1$ [14], and Φ is a scalar field in the Einstein frame defined by

$$\Phi = \frac{1}{4} \left(\frac{3 + 2\omega_{BD}}{\pi} \right)^{1/2} \ln \left(\frac{\phi}{\phi_0} \right), \quad (7)$$

$G_{\mu\nu}^{(E)}$ is the Einstein tensor defined by the metric $g_{\mu\nu}^{(E)}$, and

$$T_{\mu\nu}^{(E)} = \frac{1}{\phi_0} \exp \left[-4 \left(\frac{\pi}{3 + 2\omega_{BD}} \right)^{1/2} \Phi \right] T_{\mu\nu} \quad (8)$$

$$T^{(E)} = \frac{1}{\phi_0} \exp \left[-8 \left(\frac{\pi}{3 + 2\omega_{BD}} \right)^{1/2} \Phi \right] T \quad (9)$$

$$T_{\mu\nu}^{(\Phi)} = \nabla_\mu \Phi \nabla_\nu \Phi - \frac{1}{2} g_{\mu\nu}^{(E)} (\nabla^{(E)} \Phi)^2. \quad (10)$$

From these equations, it is easy to see that any vacuum solutions in Einstein theory are equivalent with those in BD theory with $\Phi = \text{constant}$. In particular, the Kerr solution with $\Phi = 0$ is a solution in BD theory as well.

We now discuss gravitational waves emitted by a test particle plunging into a Kerr black hole. In order to calculate the waveform of emitted gravitational radiation and its energy, we perturb the Kerr background spacetime. Since we are interested in a test particle motion, we adopt the matter Lagrangian as

$$S_{matter} = \int d\tau \mu(\phi), \quad (11)$$

where τ and μ are proper time and mass of a test particle, respectively. In the case that the self-gravity of the test particle cannot be ignored, for example an extrapolation of a test particle into a neutron star or a black hole, μ should depend on the BD scalar ϕ , which does not guarantee that the test particle moves along the geodesic and the gravitational weak equivalence principle is no longer valid (Nordtvert effect). In this paper, however, we consider only the case of $\mu=\text{constant}$ just for simplicity. When we extrapolate our results into the case of the direct collision of two compact objects, we should take into account the ϕ -dependence in μ [8], but the difference may not be so large unless the test particle is a black hole, in which case scalar gravitational waves will not be emitted, at least within the linear perturbation approximation [17]. The energy-momentum tensor of the test particle is now

$$T^{\mu\nu} = \frac{\mu}{\sqrt{-g}} \int d\tau \frac{dz^\mu}{d\tau} \frac{dz^\nu}{d\tau} \delta^{(4)}(x - z(\tau)), \quad (12)$$

where $z^\mu(\tau)$ is the geodesic of a test particle.

Now we linearize our basic equations in the Einstein frame around a background vacuum spacetime :

$$g_{\mu\nu}^{(E)} = g_{\mu\nu}^{(0)} + h_{\mu\nu}^{(E)} \quad \text{and} \quad \Phi = \Phi^{(0)} + \Phi^{(1)}, \quad (13)$$

where $\Phi^{(0)} = 0$. Then the first order perturbation equations are

$$G_{\mu\nu}^{(1)}[h_{\alpha\beta}^{(E)}] = 8\pi T_{\mu\nu}^{(E)}[\mu, g_{\mu\nu}^{(0)}, \Phi^{(0)} = 0] \quad (14)$$

$$\square^{(0)}\Phi^{(1)} = 2 \left(\frac{\pi}{3 + 2\omega_{BD}} \right)^{1/2} T^{(E)}[\mu, g_{\mu\nu}^{(0)}, \Phi^{(0)} = 0], \quad (15)$$

where

$$G_{\mu\nu}^{(1)}[h_{\alpha\beta}^{(E)}] = \frac{1}{2} \left[-\nabla_{\mu}^{(0)} \nabla_{\nu}^{(0)} h^{(E)} - \nabla_{\alpha}^{(0)} \nabla^{(0)\alpha} h_{\mu\nu}^{(E)} + \nabla_{\nu}^{(0)} \nabla^{(0)\alpha} h_{\alpha\mu}^{(E)} + \nabla_{\mu}^{(0)} \nabla^{(0)\alpha} h_{\alpha\nu}^{(E)} - g_{\mu\nu}^{(0)} \left(-\nabla_{\alpha}^{(0)} \nabla^{(0)\alpha} h^{(E)} + \nabla^{(0)\alpha} \nabla^{(0)\beta} h_{\alpha\beta}^{(E)} \right) \right] \quad (16)$$

is the first order perturbation of the Einstein tensor $G_{\mu\nu}$ and $\square^{(0)}$ denotes the D'Alembertian of the background spacetime. Since mass of the test particle μ is a first order quantity, both energy-momentum tensors in Einstein frame and in Jordan-Brans-Dicke frame differ only by a constant factor $1/\phi_0$ in the linear perturbation equations (14), (15). We also find that the metric perturbation equation (14) for $h_{\mu\nu}^{(E)}$ is exactly the same as those in Einstein theory [18].

In the Jordan-Brans-Dicke frame, the perturbation variables, which are expanded as

$$g_{\mu\nu} = g_{\mu\nu}^{(0)} + h_{\mu\nu} \quad \text{and} \quad \phi = \phi_0 + \phi^{(1)}, \quad (17)$$

are given by the variables in the Einstein frame as

$$h_{\mu\nu} = h_{\mu\nu}^{(E)} - g_{\mu\nu}^{(0)} \frac{\phi^{(1)}}{\phi_0} \quad \text{and} \quad \frac{\phi^{(1)}}{\phi_0} = 4 \left(\frac{\pi}{3 + 2\omega_{BD}} \right)^{1/2} \Phi^{(1)}. \quad (18)$$

For the equation for $\phi^{(1)}$, from Eq. (15) or (3), we obtain

$$\square^{(0)} \phi^{(1)} = \frac{8\pi}{3 + 2\omega_{BD}} T. \quad (19)$$

As for the metric perturbations in the Jordan-Brans-Dicke frame, we just have to study the perturbations and gravitational waves in Einstein theory, since the basic equations in the Einstein frame are exactly the same as those in the Einstein theory, which we have better knowledge in treating in ordinary procedures.

III. GRAVITATIONAL WAVES FROM TEST PARTICLES FALLING INTO KERR BLACK HOLE

A. Metric Perturbations

We start considering a test particle motion in the Kerr background spacetime and analyze first the tensor modes of its gravitational waves (TGWs) emitted by a plunging test particle. In order to use these results in the analysis in §4, we take into account a test particle not only moving in the equatorial plane but also moving off the equatorial plane, which results have not been obtained so far. This means that we will also present new results in Einstein theory, i.e., the waveforms and energy flux in the case of test particles falling with a constant azimuthal angle into a Kerr black hole.

Let us begin from a brief review of a black hole perturbation analysis in Einstein theory, which gives the same results for tensor modes in BD theory up to a factor $1/\phi_0$. In order to calculate metric perturbations of a Kerr spacetime in the Einstein theory, we adopt the Sasaki-Nakamura formalism [19], in which the Regge-Wheeler equation is generalized by a transformation from the Teukolsky equation [20]. The radial wave equation becomes

$$\left[\frac{d^2}{dr^{*2}} - F(r) \frac{d}{dr^*} - U(r) \right] X_{lm\omega}(r) = S_{lm\omega}(r), \quad (20)$$

where the tortoise coordinate r^* is defined as

$$dr^* = \frac{r^2 + a^2}{\Delta} dr. \quad (21)$$

with $\Delta = r^2 - 2Mr + a^2$. The potential functions $F(r)$ and $U(r)$ are given as

$$F(r) = \frac{\Delta}{r^2 + a^2} \frac{1}{\gamma} \frac{d\gamma}{dr},$$

$$U(r) = G^2 - FG + \frac{\Delta}{(r^2 + a^2)} \frac{dG}{dr} + \frac{\Delta}{(r^2 + a^2)^2} U_1,$$

with

$$\begin{aligned}
\gamma(r) &= c_0 + \frac{c_1}{r} + \frac{c_2}{r^2} + \frac{c_3}{r^3} + \frac{c_4}{r^4}, \\
c_0 &= -12iM\omega + \lambda(\lambda + 2) + 12a\omega(m - a\omega), \\
c_1 &= 8ia[3a\omega - \lambda(m - a\omega)], \\
c_2 &= 24iaM(m - a\omega) + 12a^2[1 - 2(m - a\omega)^2], \\
c_3 &= 24ia^3(m - a\omega) - 24Ma^2, \\
c_4 &= 12a^4, \\
G(r) &= -\frac{1}{r^2 + a^2} \frac{d\Delta}{dr} + \frac{r\Delta}{(r^2 + a^2)^2}, \\
U_1(r) &= V_T + \frac{\Delta^2}{\beta} \left[\frac{d}{dr} \left(2\alpha + \frac{d\beta/dr}{\Delta} \right) - \frac{d\gamma/dr}{\gamma} \left(\alpha + \frac{d\beta/dr}{\Delta} \right) \right], \\
\alpha &= -i\frac{K\beta}{\Delta^2} + 3i\frac{dK}{dr} + \lambda + \frac{6\Delta}{r^2}, \\
\beta &= 2\Delta \left(-iK + r - M - \frac{2\Delta}{r} \right).
\end{aligned}$$

V_T is the potential in the Teukolsky equation, which is given as

$$V_T(r) = -\frac{K^2 + 4i(r - M)K}{\Delta} + 8i\omega r + \lambda, \quad (22)$$

where $K = (r^2 + a^2)\omega - ma$. In Appendix A, we present the explicit form of the source term $S_{lm\omega}(r)$ for the general motion of a test particle.

To describe the wave function $X_{lm\omega}(r)$ of Eq. (20) using the Green function method, we need two independent homogeneous solutions of the Sasaki-Nakamura equation, i.e.,

$$\begin{aligned}
X_{lm\omega}^{in(0)}(r) &= \begin{cases} e^{-ikr^*} & r^* \rightarrow -\infty \\ A_{lm\omega}^{in} e^{-i\omega r^*} + A_{lm\omega}^{out} e^{i\omega r^*} & r^* \rightarrow \infty \end{cases}, \\
X_{lm\omega}^{out(0)}(r) &= \begin{cases} B_{lm\omega}^{in} e^{-ikr^*} + B_{lm\omega}^{out} e^{ikr^*} & r^* \rightarrow -\infty \\ e^{i\omega r^*} & r^* \rightarrow \infty \end{cases},
\end{aligned}$$

where $k = \omega - ma/2r_+$ with $r_+ = M + \sqrt{M^2 - a^2}$ being the radius of the event horizon, and the Wronskian $W^{(TGW)}$

$$W^{(TGW)} \equiv X_{lm\omega}^{in(0)} \frac{dX_{lm\omega}^{out(0)}}{dr^*} - X_{lm\omega}^{out(0)} \frac{dX_{lm\omega}^{in(0)}}{dr^*} = 2i\omega A_{lm\omega}^{in} \frac{\gamma}{c_0}.$$

Then the inhomogeneous solution of Eq. (20) becomes

$$X_{lm\omega}(r) = X_{lm\omega}^{in(0)} \int_{r^*}^{\infty} \frac{S_{lm\omega}(r)}{W^{(TGW)}} X_{lm\omega}^{out(0)} dr^* + X_{lm\omega}^{out(0)} \int_{-\infty}^{r^*} \frac{S_{lm\omega}(r)}{W^{(TGW)}} X_{lm\omega}^{in(0)} dr^*.$$

For observation, we only have to know the asymptotic behavior of the wave function $X_{lm\omega}(r)$ at infinity, which is

$$X_{lm\omega}^{(\infty)}(r) = A_{lm\omega}^{(\infty)} e^{i\omega r^*}, \quad (23)$$

where

$$A_{lm\omega}^{(\infty)} = \frac{c_0}{2i\omega A_{lm\omega}^{in}} \int_{-\infty}^{\infty} \frac{S_{lm\omega}(r)}{\gamma} X_{lm\omega}^{in(0)}(r) dr^*. \quad (24)$$

Then the waveform at infinity is

$$h_+ - ih_\times = \frac{8}{r} \int_{-\infty}^{\infty} d\omega e^{i\omega(r^*-t)} \sum_{l,m} \frac{A_{lm\omega}^{(\infty)}}{c_0} {}_{-2}S_{lm}^{a\omega}(\theta) \frac{e^{im\varphi}}{\sqrt{2\pi}}, \quad (25)$$

where ${}_sS_{lm}^{a\omega}(\theta)$ is a spin-weighted spheroidal function, which obeys

$$\left[\frac{1}{\sin\theta} \frac{d}{d\theta} \left(\sin\theta \frac{d}{d\theta} \right) - \left(a^2\omega^2 \sin^2\theta + \frac{(m+s\cos\theta)^2}{\sin^2\theta} + 2a\omega s \cos\theta - s - 2am\omega - \lambda \right) \right] {}_sS_{lm}^{a\omega}(\theta) = 0, \quad (26)$$

with $s = -2, -1, 0, 1$ or 2 and λ being the eigenvalue. ${}_sS_{lm}^{a\omega}(\theta)$ is normalized as

$$\int_0^\pi d\theta \sin\theta |{}_sS_{lm}^{a\omega}(\theta)|^2 = 1.$$

From Eq. (25), the energy flux of gravitational waves at infinity becomes

$$\begin{aligned} \frac{dE^{(\text{TGW})}}{dt} &= \frac{r^2}{32\pi} \int \frac{\partial h_{TT}^{ij}}{\partial t} \frac{\partial h_{TT}^{ij}}{\partial t} d\Omega \\ &= \frac{4}{\pi} \sum_{l,m} \left| \int_{-\infty}^{\infty} d\omega \omega \frac{A_{lm\omega}^{(\infty)}}{c_0} e^{i\omega(r^*-t)} \right|^2. \end{aligned} \quad (27)$$

Then, the total energy and the energy spectrum of the TGW are given as

$$E^{(\text{TGW})} = \int_{-\infty}^{\infty} d\omega \sum_{l,m} \left(\frac{dE^{(\text{TGW})}}{d\omega} \right)_{lm\omega}, \quad (28)$$

and

$$\left(\frac{dE^{(\text{TGW})}}{d\omega} \right)_{lm\omega} = 8\omega^2 \left| \frac{A_{lm\omega}^{(\infty)}}{c_0} \right|^2, \quad (29)$$

respectively.

Solving this equation, Kojima and Nakamura [21] analyzed the gravitational radiation induced by a test particle with mass μ and angular momentum L_z plunging on the equatorial plane or along the rotation axis into a Kerr black hole with mass M and angular momentum $J = Ma$. They calculated the waveform (only h_+ mode) and the emitted energy. They pointed out that the behaviors are similar to those of a Schwarzschild black hole but the amplitude becomes larger as the rotation parameter a gets larger. They showed that the emitted energy from the particle moving along the axis is smaller than that from the particle

moving on the equatorial plane. They also calculated the total energy, linear momentum and angular momentum extracted from the system by gravitational radiation and showed that all of them become larger as the rotation of black hole gets faster.

For TGWs in BD theory, we have to multiply $1/\phi_0$ by the energy momentum tensor, and then the energy flux. But since $1 \leq \phi_0 < 1.001$ for $\omega_{BD} > 500$, we may ignore such a factor here. In order to compare the tensor modes with the scalar mode, we calculate the waveform and emitted energy of gravitational radiation induced by a test particle plunging with a constant azimuthal angle into a Kerr black hole. The particle motion with a constant azimuthal angle is a geodesic in Kerr spacetime, if $E = \mu$ and $L_z = 0$, which we assume here (see Appendix). We have analyzed such a special geodesic because in the next section we will use it in the analysis of non-spherical dust shell collapse. We wish to emphasize that the results with the azimuthal angle $\theta \neq 0$ or $\neq \pi/2$ are new even in Einstein theory [22]. We have checked our numerical codes with the latest results, Mino, Shibata and Tanaka [23].

We show the emitted waveforms and emitted energy for several values of the Kerr parameter a ($a = 0, 0.5, 0.9, 0.99$) and of the azimuthal angle θ ($\theta = \pi/6, \pi/3, \pi/2$ (the equatorial plane)) in Figs. 1 and 2. We assume that the observer is in the position of $\theta = \pi/2$, $\phi = 0$. One of the important results is that only in the case of an observer perpendicular to the direction of a direct collision, and for very small rotation of compact objects, do we find little gravitational radiation (Fig. 1 $a = 0$ case). This is consistent with a full numerical analysis of two black hole collision [13].

We also present the total energy of TGWs in terms of the azimuthal angle in Fig. 2. The emitted energy changes smoothly in terms of the azimuthal angle from the largest one for $\theta = \pi/2$ to the smallest one for $\theta = 0$, each values are found in [21] and [27].

B. Scalar Perturbations

Next we consider the scalar mode $\phi^{(1)}$ of the perturbation. We expand $\phi^{(1)}$ using spin-weighted spheroidal function as

$$\phi^{(1)} = \sum_{l,m} \int d\omega e^{-i\omega t} \frac{Z_{lm\omega}(r)}{\sqrt{r^2 + a^2}} {}_0S_{lm}^{a\omega}(\theta) \frac{e^{im\varphi}}{\sqrt{2\pi}}, \quad (30)$$

then, from the field equation (19), the radial wave function $Z_{lm\omega}(r)$ obeys the differential equation

$$\left[\frac{d^2}{dr^{*2}} + V(r) \right] Z_{lm\omega}(r) = \frac{8\pi}{2\omega_{BD} + 3} \frac{\Delta}{(r^2 + a^2)^{3/2}} T_{lm\omega}(r), \quad (31)$$

where the potential $V(r)$ is given by

$$V(r) = \left(\omega - \frac{am}{r^2 + a^2} \right)^2 - \frac{\Delta[\lambda(r^2 + a^2)^2 + (2Mr^3 + a^2r^2 - 4Ma^2r + a^4)]}{(r^2 + a^2)^4}, \quad (32)$$

and the trace of energy momentum tensor is expanded as

$$\Sigma T = \sum_{l,m} \int d\omega e^{-i\omega t} T_{lm\omega}(r) {}_0S_{lm}^{a\omega}(\theta) \frac{e^{im\varphi}}{\sqrt{2\pi}}, \quad (33)$$

with $\Sigma = r^2 + a^2 \cos^2 \theta$. We find that

$$T_{lm\omega}(r) = -\frac{1}{(2\pi)^{3/2}} \left| \frac{d\tau(r)}{dr} \right| e^{i(\omega t(r) - m\varphi(r))} {}_0S_{lm}^{a\omega}(\theta(r)), \quad (34)$$

where we have to insert a test particle orbit described in terms of r , i.e., $z^\mu = (t(r), r, \theta(r), \varphi(r))$. We again use the Green function method to derive the wave function $Z_{lm\omega}(r)$. Defining two independent homogeneous solutions as

$$\begin{aligned} Z_{lm\omega}^{in(0)}(r) &= \begin{cases} e^{-ikr^*} & r^* \rightarrow -\infty \\ C_{lm\omega}^{in} e^{-i\omega r^*} + C_{lm\omega}^{out} e^{i\omega r^*} & r^* \rightarrow \infty \end{cases}, \\ Z_{lm\omega}^{out(0)}(r) &= \begin{cases} D_{lm\omega}^{in} e^{-ikr^*} + D_{lm\omega}^{out} e^{ikr^*} & r^* \rightarrow -\infty \\ e^{i\omega r^*} & r^* \rightarrow \infty \end{cases}, \end{aligned}$$

and the Wronskian $W^{(SGW)}$

$$W^{(SGW)} \equiv Z_{lm\omega}^{in(0)} \frac{dZ_{lm\omega}^{out(0)}}{dr^*} - Z_{lm\omega}^{out(0)} \frac{dZ_{lm\omega}^{in(0)}}{dr^*} = 2i\omega C_{lm\omega}^{in},$$

the inhomogeneous solution of Eq. (31) is given as

$$\begin{aligned} Z_{lm\omega}(r) &= \frac{8\pi}{2\omega_{BD} + 3} \frac{1}{W^{(SGW)}} \left(Z_{lm\omega}^{in(0)} \int_{r^*}^{\infty} \frac{\Delta}{(r^2 + a^2)^{3/2}} T_{lm\omega}(r) Z_{lm\omega}^{out(0)} dr^* \right. \\ &\quad \left. + Z_{lm\omega}^{out(0)} \int_{-\infty}^{r^*} \frac{\Delta}{(r^2 + a^2)^{3/2}} T_{lm\omega}(r) Z_{lm\omega}^{in(0)} dr^* \right). \end{aligned}$$

We only need the asymptotic behavior of the wave function $Z_{lm\omega}(r)$ at infinity for observation, which is

$$Z_{lm\omega}^{(\infty)}(r) = C_{lm\omega}^{(\infty)} e^{i\omega r^*}, \quad (35)$$

where

$$C_{lm\omega}^{(\infty)} = \frac{1}{2i\omega C_{lm\omega}^{in}} \int_{-\infty}^{\infty} \frac{\Delta}{(r^2 + a^2)^{3/2}} T_{lm\omega}(r) Z_{lm\omega}^{in(0)}(r) dr^*. \quad (36)$$

Then the waveform at infinity is derived as

$$\phi^{(1)} = \frac{1}{\sqrt{r^2 + a^2}} \int_{-\infty}^{\infty} d\omega e^{i\omega(r^* - t)} \sum_{l,m} C_{lm\omega}^{(\infty)} {}_0S_{lm}^{a\omega}(\theta) \frac{e^{im\varphi}}{\sqrt{2\pi}}. \quad (37)$$

The energy flux of the SGW observed at infinity is defined as [16]

$$\frac{dE^{(SGW)}}{dt} = \frac{(2\omega_{BD} + 3)^2}{32\pi(\omega_{BD} + 2)} \int \left(\frac{\partial \phi}{\partial t} \right)^2 dS. \quad (38)$$

Then the total energy $E^{(\text{SGW})}$ is now

$$E^{(\text{SGW})} = \sum_{l,m} \int_{-\infty}^{\infty} d\omega \left(\frac{dE^{(\text{SGW})}}{d\omega} \right)_{lm\omega}, \quad (39)$$

with

$$\left(\frac{dE^{(\text{SGW})}}{d\omega} \right)_{lm\omega} = \frac{(2\omega_{BD} + 3)^2}{16(\omega_{BD} + 2)} \omega^2 |C_{lm\omega}^{(\infty)}|^2. \quad (40)$$

In order to check our numerical code, for the case of a test particle falling into Schwarzschild background, we have compared our results with those by Shibata, Nakao and Nakamura [12], finding a good agreement. We show our results in Figs. 3 to 6 for $a=0, 0.5, 0.9$, and 0.99 and for $\theta = \pi/6, \pi/3$ and $\pi/2$. Here we assume $\omega_{BD} = 500$. Since $\omega_{BD} \gg 1$, the amplitude and energy of the SGWs are both approximately proportional to $1/\omega_{BD}$ (see Eqs. (31) and (40)) and then we can rescale our results for any arbitrary value of ω_{BD} .

From the waveforms (Fig. 3), energy spectrum (Fig.4) and the total energy (Fig. 5), we find that the results depend only slightly on the values of a and θ . This θ independence may be understood from the fact that the s wave ($l = 0$) is dominant in the SGWs. As for the Kerr parameter, although the phase difference depends on a , we find that the waveforms themselves little depends on a . The energy spectrum has three main peaks (see Fig. 4) and the frequency of the largest peak is almost the same as that of the quasi-normal mode (QNM). These QNMs of scalar modes ($l = 0$) are obtained by Simone-Will [24] and Anderson [25] for the Schwarzschild black hole case, using WKB approximation and phase-integral method, respectively. Here, using Leaver's technique [26] of continued fractions, we derive the $l = 0$ modes of QNMs for a Kerr black hole and try to fit the tail part of the obtained waveform by them. In Fig. 6, we show both the calculated waveform (bold line) and the curve fitted by QNM (dotted line). The results show that the ringing tail of the SGW can also fit by the QNM. To draw a fitting curve, we need only the first QNM, i.e.,

$$\phi^{(1)} = \frac{A\mu}{r} e^{\text{Im}[\omega_1](t-r^*+b)} \cos(\text{Re}[\omega_1](t-r^*+b)). \quad (41)$$

with $A = -0.0012$, $b = -33$, $M\omega_1 = 0.11045 - 0.10490i$ for $a = 0$, $A = 0.0013$, $b = -39$, $M\omega_1 = 0.11251 - 0.10000i$ for $a = 0.5M$, $A = -0.0014$, $b = -72$, $M\omega_1 = 0.11380 - 0.09160i$ for $a = 0.9M$. However, the QNM fit to the ringing tail of the SGW is not as good as the fit to the TGWs. The situation does not change even if we include the higher QNMs. This may be because we cannot separate the burst part and the ringing tail part of SGWs, we cannot fit the tail part of SGW only by the QNMs.

Because of the ratio of the maximum amplitude of GW to that of SGW is 200:1, a detection of the SGW itself is usually very difficult, unless we observe the polarizations and divide the tensor and the scalar modes. Only one exceptional case is that the observer's line of sight is in the direction of a falling test particle into a Schwarzschild black hole. In this case, the SGW always dominates the tensor modes.

IV. GRAVITATIONAL WAVES FROM NON-SPHERICAL DUST SHELL COLLAPSE

As we found in the previous section, when a test particle is falling into a Kerr black hole, the ratio of maximum amplitude of SGW to TGW is 1:200. This suggests that direct detection of SGWs from a collision of compact bodies is a hard task. However, the fact that SGWs are generated even in a spherically symmetric system, while TGWs require a deviation from spherical symmetry, gives us an expectation that the SGW may become dominant in some situations such as an almost spherical supernova explosion. Since a completely spherically symmetric system is unrealistic, we may ask how much deviation is allowed for the SGW to dominate TGW. In this section, we analyze the gravitational radiation from a collapsing non-spherical dust-shell, which consists of test particles (so its self gravity is ignored), into a Kerr black hole. In early studies by Nakamura and Sasaki [27] and Shapiro and Wasserman [28], the TGWs for a deformed shell falling into a Schwarzschild black hole were investigated. Our study is an extension of their researches to a rotating black hole case and/or to BD theory.

The gravitational radiation from a dust shell is derived from a linear combination of test particles falling into a black hole. If the dust shell is spherically symmetric, a phase cancellation mechanism reduces the energy of gravitational waves to zero in the Schwarzschild black hole case.

Let us begin by defining the shape of a dust shell by a function $r = r_i(\theta)$ ($i = 1, 2$);

$$r_1(\theta) = r_0(1 + \delta \cos^2 \theta) \quad (\delta \geq 0) \quad (\text{prolate}), \quad (42)$$

$$r_2(\theta) = r_0(1 + \delta \sin^2 \theta) \quad (\delta \geq 0) \quad (\text{oblate}), \quad (43)$$

where δ is a parameter which denotes a deviation from a spherically symmetric dust shell and r_0 is a typical radius of the shell.

In the case of a Schwarzschild black hole, test particle motion with zero angular momentum does not depend on the azimuthal angle θ , and the dynamics of particles in the shell can be replaced by that on the equatorial plane. This fact makes our calculation of energy of gravitational waves easy as follows. Using the shape function $r_i(\theta)$, we introduce a correction function $f_{lm\omega}$ [27,29] as

$$f_{lm\omega} = \frac{1}{2} \int_0^\pi d\theta \sin \theta e^{i\omega[t(r_0) - t(r_i(\theta))]} P_l(\theta) \delta_{m0}, \quad (44)$$

where P_l is the Legendre function and $t(r)$ is the coordinate time when the particle comes to a position r . Then we define the source term $S_{lm\omega}$ and wave function $X_{lm\omega}$ for non-spherical dust collapse from those of test particles as

$$S_{lm\omega}^{[\text{shell}]} = f_{lm\omega} S_{lm\omega}^{[\text{particle}]}, \quad (45)$$

$$X_{lm\omega}^{[\text{shell}]} = f_{lm\omega} X_{lm\omega}^{[\text{particle}]}. \quad (46)$$

We then obtain a total energy of gravitational radiation from non-spherical dust shell collapse as

$$E^{(\text{TGW})} = \sum_{l,m} \int_{-\infty}^{\infty} d\omega \left(\frac{dE^{(\text{TGW})}}{d\omega} \right)_{lm\omega} \quad (47)$$

where

$$\begin{aligned} \left(\frac{dE^{(\text{TGW})}}{d\omega} \right)_{lm\omega} &= |f_{lm\omega}|^2 \left(\frac{dE^{(\text{TGW})}}{d\omega} \right)_{lm\omega}^{[\text{particle}]} \\ &= 8\omega^2 |f_{lm\omega}|^2 \left| \frac{X_{lm\omega}^{(\infty)[\text{particle}]} }{c_0} \right|^2. \end{aligned} \quad (48)$$

As for the SGW, we have

$$E^{(\text{SGW})} = \sum_{l,m} \int_{-\infty}^{\infty} d\omega \left(\frac{dE^{(\text{SGW})}}{d\omega} \right)_{lm\omega} \quad (49)$$

where

$$\left(\frac{dE^{(\text{SGW})}}{d\omega} \right)_{lm\omega} = \frac{(2\omega_{BD} + 3)^2}{16(\omega_{BD} + 2)} \omega^2 |f_{lm\omega}|^2 |Z_{lm\omega}^{(\infty)[\text{particle}]}|^2. \quad (50)$$

In a Kerr spacetime, however, we cannot adopt this simple formula because the radial wave function depends on the azimuthal angle θ , which means that we cannot factorize a correction function as Eq. (48). In this case, we have to calculate the total energy by summing up test particles. Therefore, as for test particles of the dust shell, we choose $E = \mu$ and $L_z = 0$, for which a trajectory of $\theta = \text{constant}$ becomes a geodesic. First, using Eq. (29), we prepare the wave function from a test particle with constant θ , which we denote $X_{lm\omega}(r; \theta)$. Then we calculate the energy spectrum of the TGW as

$$\left(\frac{dE^{(\text{TGW})}}{d\omega} \right)_{lm\omega} = 2\omega^2 \left| \int_0^\pi d\theta \sin \theta \frac{X_{lm\omega}^{(\infty)}(r; \theta)}{c_0} e^{i\omega[t(r_0) - t(r_i(\theta))]} \right|^2 \delta_{m0}, \quad (51)$$

where $X_{lm\omega}^{(\infty)}(r; \theta)$ is the asymptotic form of $X_{lm\omega}(r; \theta)$ at infinity. To evaluate the integration (51), we prepare data at 60 points for θ in $[0, \pi]$. The total energy is given by Eq. (47).

As for the SGW, we also find

$$\begin{aligned} \left(\frac{dE^{(\text{SGW})}}{d\omega} \right)_{lm\omega} &= \frac{(2\omega_{BD} + 3)^2}{16(\omega_{BD} + 2)} \\ &\times \omega^2 \left| \int_0^\pi d\theta \sin \theta Z_{lm\omega}^{(\infty)}(r; \theta) e^{i\omega[t(r_0) - t(r_i(\theta))]} \right|^2 \delta_{m0}. \end{aligned} \quad (52)$$

We show our results in Figs. 7 and 8. For a Schwarzschild background, Nakamura and Sasaki [27] calculated the total energy of TGWs from a dust shell and pointed out that the energy will be generated maximally for a deviation of $\delta_{cr}^{(\text{TGW})} \sim 0.5$ from spherical symmetry. The reason is that if the dust shell is close to a spherical symmetry, the TGW will not be generated so much while if the deviation is larger than $\delta_{cr}^{(\text{TGW})}$, a phase cancellation effect will also reduce the emitted energy [27].

For the case of SGW, we find that the energy does not depend on the deformation parameter δ if δ is smaller than some critical value ($\delta_{cr}^{(SGW)} = 1.5$) (see Fig. 7). This is understood by the fact that the $l=0$ mode is dominant for the SGW. Beyond the critical value, the above cancellation effect also reduces the energy of the SGWs. At the critical deviation, the time lag between the longest and shortest radii is almost the same as the most dominant QNM period. If the deviation is larger than the critical value, i.e., if the time lag is larger than the most dominant QNM period, the total energy is reduced by a phase cancellation. In fact, the difference between the values of $\delta_{cr}^{(TGW)}$ and $\delta_{cr}^{(SGW)}$ is explained by the difference between QNM periods of TGWs and SGWs.

For the case of a rotating black hole, we show the results in Fig. 8. The results are similar to those of the Schwarzschild case except for the following two points. First, since the system is not completely spherically symmetric, the TGW is also generated for any values of δ . There exists some value of δ_0 , which is not zero and depends on the rotation parameter a (e.g. $\delta_0 \sim 0.02$ for $a = 0.5$, $\delta_0 \sim 0.08$ for $a = 0.9$, and $\delta_0 \sim 0.10$ for $a = 0.99$), at which the emitted energy of TGWs takes a minimum value. As a increases, its minimum energy and the corresponding deformation parameter δ_0 increase (see Fig. 8(b)). The increase of minimum energy is easily understood because of a large deviation from spherical symmetry. The fact that δ_0 increases as a increases may also be explained by the following reason. When we estimate the falling time of a test particle from a finite radius in a Kerr spacetime, the time along the rotation axis is longer than that on the equatorial plane if the initial radii are equal. Then if the dust shell is slightly oblate, the time lag between test particles along the rotation axis and on the equatorial plane becomes smaller, which is close to a spherically symmetric case, and then a phase cancellation effect will reduce the emitted gravitational radiation. As for the SGW in a Kerr geometry, the results are almost same as those in a Schwarzschild one.

Secondly, the existence of a non-vanishing minimum value of TGW is important for observation. Since the SGW does not depend on δ , we can find how much deviation is allowed for SGW to dominate TGW from Figs. 7 and 8. That is, the energy of the SGW is larger than that of the TGW if $\delta_1 < \delta < \delta_2$ and $\omega_{BD} = 500$ ($\delta_1 = -0.07$, $\delta_2 = 0.07$ for $a = 0$, $\delta_1 = -0.05$, $\delta_2 = 0.09$ for $a = 0.5$, $\delta_1 = 0.03$, $\delta_2 = 0.11$ for $a = 0.9$, and $\delta_1 = 0.05$, $\delta_2 = 0.12$ for $a = 0.99$ when $\omega_{BD} = 500$). The emitted SGW is proportional to $1/\omega_{BD}$ if $\omega_{BD} \gg 1$. Then if ω_{BD} is larger than some critical value ω_{BD}^{cr} , which depends on a , the SGWs never dominate TGWs ($\omega_{BD}^{cr} = 20,000$ for $a = 0.5$, $\omega_{BD}^{cr} = 1,250$ for $a = 0.9$, and $\omega_{BD}^{cr} = 750$ for $a = 0.99$). We may speculate that in generic gravitational collapse the SGW does not dominate the TGWs if $\omega_{BD} >$ several thousand.

V. CONCLUDING REMARKS

In this paper, analyzing test particles around a Kerr black hole, we studied both scalar and tensor modes of gravitational waves in BD theory. We examined two models: A test particle plunging with a constant azimuthal angle into a Kerr black hole, and a non-spherical dust shell collapsing into a Kerr black hole. In the first model, we show that the SGWs have little dependence on the the rotation parameter a and the azimuthal angle θ because the s -wave is dominant. If a coupling constant of BD theory $\omega_{BD} \gtrsim 500$, however, the TGWs

dominate the SGWs except for one very limited case, that is, an observation in the face-on direction of a test particle falling into a Schwarzschild black hole. In the second model, we also show that the SGWs dominate only for the highly spherically symmetric case. In particular, for the case of a rotating black hole, the emitted energy for TGWs takes a non-zero minimum value when the deformation is slightly oblate. Since that for SGW is less sensitive to a deviation from a spherical symmetry, the SGW cannot be dominant unless $\omega_{BD} \lesssim 750$ for $a/M = 0.99$ or unless $\omega_{BD} \lesssim 20,000$ for $a/M = 0.5$.

Here, we remark on the detectability of SGWs. In the First/Advanced LIGO operation, the observation limit of the gravitational wave amplitude is expected to be $h > 10^{-21}$ for the 50 ~ 200 Hz band, and $h > 10^{-23}$ for the 10 ~ 1,000 Hz band, respectively [3].

First we mention that the QNM frequency provides some naive measure for the observable range. The relationship between the observed frequency f and the QNM frequency ω is

$$f \simeq 3.30 \times 10^3 \left(\frac{M_\odot}{M} \right) M\omega \quad [\text{Hz}]. \quad (53)$$

for typical observation of NS ($M \simeq 1.4M_\odot$) and BH ($M \sim 10M_\odot$). The most dominant contribution of QNMs is $n = 1$, for which we find $\text{Re } M\omega \sim 0.37$ for TGW and $\text{Re } M\omega \sim 0.11$ for SGW. Hence, for the BH-NS system, the observable frequencies in First (Advanced) LIGO are $M\omega = 0.02 \sim 0.08$ ($0.004 \sim 0.4$), while for the BH-BH system, $0.15 \sim 0.61$ ($0.03 \sim 3.04$). Both observations of SGW and TGW are within preferable ranges of frequency.

Secondly, we estimate the maximum amplitude of gravitational radiation. The expected amplitudes of SGW and TGWs ($h^{(\text{TGW})}, h^{(\text{SGW})}$) are

$$\begin{aligned} h^{(\text{TGW})} &\simeq 2 \times 10^{-20} \left(\frac{\mu}{M} \right) \left(\frac{1\text{Mpc}}{r} \right), \\ h^{(\text{SGW})} &\simeq 1 \times 10^{-22} \left(\frac{500}{\omega_{BD}} \right) \left(\frac{\mu}{M} \right) \left(\frac{1\text{Mpc}}{r} \right), \end{aligned}$$

where we set $h_+ = 0.4$ and $\phi^{(1)} = 0.002$ from our results.

Fixing the BD coupling constant $\omega_{BD} = 500$, we find that the limiting distance of SGWs in First LIGO for NS-NS, BH-BH collision is $r=100\text{kpc}$, while $r=20\text{Mpc}$ for TGWs. This limiting distance becomes much longer when we have the NS-BH system and Advanced LIGO detector, i.e., the target for SGW could set farther than the Virgo Cluster (20Mpc).

Conversely, if the SGW is observed in a gravitational wave detector with polarization information, what kind of constraint on the BD coupling constant ω_{BD} we will find? We can at least discuss the upper bound. For example, we can easily say that if NS-BH collision occurred in our Galaxy and the SGW were observed, we could determine definitely the BD coupling constant even for much higher values than 500 (see Table 1).

Although our analysis has been done by test particles, we believe that our conclusions for the SGWs are valid for more generic cases. As for other scalar-tensor theories of gravity, we expect similar results, although we may need further analysis [30]. In order to determine a theory of gravity by gravitational wave detection, the above results require observations of polarizations and extractions of information of the scalar mode from observed data, for which we need several observational sites in the world.

It is very interesting to test theories of gravity by direct observation of gravitational radiation. It will open a new window in gravitational astronomy, which may provide a third

and the final observational eye to see the Universe and may be expected to reveal some problems in fundamental physics (such as the equation of state at high density) as well as to determine many properties and orbital elements of compact objects.

ACKNOWLEDGMENTS

We would like to thank Takashi Nakamura, Masaru Shibata and Hideyuki Tagoshi for useful comments. We also would like to thank Paul Haines for critical reading of our manuscript. This work was supported partially by the Grant-in-Aid for Scientific Research Fund of the Ministry of Education, Science and Culture (Specially Promoted Research No. 08102010), and by a Waseda University Grant for Special Research Projects.

APPENDIX A: SOURCE TERM OF GRAVITATIONAL WAVES BY A TEST PARTICLE IN A KERR SPACETIME

In §. 2, we summarize the tensor gravitational waves from a test particle in a Kerr spacetime. In order to solve the basic equation (the Sasaki-Nakamura equation), we first have to give the source term $S_{lm\omega}$ in Eq. (20). Nakamura and Sasaki gave the explicit form for a test particle moving on the rotation axis [19] and Kojima and Nakamura gave it on the equatorial plane [21]. Shibata presented it for a motion with $r = \text{constant}$ [31]. However, no one has so far written it down for generic motions. Since we had to calculate the case with off-plane motion ($\theta = \text{constant}$), here we present the explicit form of a source term for generic motions in use of numerical calculation. Here we consider only non-periodic motion or unbound system. If the system is bounded, we may find many turning points, for which our expression is no longer valid. We have to rewrite the orbital motion in terms of time (either a coordinate time t or a proper time τ) instead of r . This may be straightforward [22].

A test particle in a Kerr spacetime is described by the equations of motion as

$$\Sigma \frac{dr}{d\tau} = \pm \sqrt{R}, \quad (\text{A1})$$

$$\Sigma \frac{d\theta}{d\tau} = \pm \sqrt{\Theta}, \quad (\text{A2})$$

$$\Sigma \frac{d\varphi}{d\tau} = - \left(aE - \frac{L_z}{\sin^2 \theta} \right) + \frac{a}{\Delta} P, \quad (\text{A3})$$

$$\Sigma \frac{dt}{d\tau} = -a(aE \sin^2 \theta - L_z) + \frac{r^2 + a^2}{\Delta} P, \quad (\text{A4})$$

where

$$P = E(r^2 + a^2) - aL_z, \quad (\text{A5})$$

$$R = P^2 - \Delta \left(r^2 + (L_z - aE)^2 + C \right), \quad (\text{A6})$$

$$\Theta = C - \cos^2 \theta \left(a^2(\mu^2 - E^2) + \frac{L_z^2}{\sin^2 \theta} \right), \quad (\text{A7})$$

and E and L_z are conserved energy and z -component angular momentum of a test particle, respectively, and C is the Carter constant. We can easily see that $\theta = \text{constant}$ is a geodesic if $E = \mu$ and $L_z = 0$.

The source term $S_{lm\omega}$ is given by

$$S_{lm\omega} = \frac{\gamma \Delta}{(r^2 + a^2)^{3/2} r^2} \mathcal{W} \exp(-i \int_r^r \frac{K}{\Delta} dr). \quad (\text{A8})$$

Here \mathcal{W} is divided into three parts as

$$\mathcal{W} = \mathcal{W}_{nn} + \mathcal{W}_{\bar{m}n} + \mathcal{W}_{\bar{m}\bar{m}}, \quad (\text{A9})$$

$$\mathcal{W}_{nn} = f_0(r) e^{i\chi(r)} + \int_r^\infty dr' f_1(r') e^{i\chi(r')} + \int_r^\infty dr' \int_{r'}^\infty dr'' f_2(r'') e^{i\chi(r'')}, \quad (\text{A10})$$

$$\mathcal{W}_{\bar{m}n} = g_0(r) e^{i\chi(r)} + \int_r^\infty dr' g_1(r') e^{i\chi(r')} + \int_r^\infty dr' \int_{r'}^\infty dr'' g_2(r'') e^{i\chi(r'')}, \quad (\text{A11})$$

$$\mathcal{W}_{\bar{m}\bar{m}} = h_0(r) e^{i\chi(r)} + \int_r^\infty dr' h_1(r') e^{i\chi(r')} + \int_r^\infty dr' \int_{r'}^\infty dr'' h_2(r'') e^{i\chi(r'')}, \quad (\text{A12})$$

where

$$\chi = \omega(t + r^*) - m\tilde{\varphi}, \quad (\text{A13})$$

$$f_0 = -\frac{1}{\omega^2} w_{nn}, \quad (\text{A14})$$

$$f_1 = -\frac{2}{\omega^2} \left(\frac{dw_{nn}}{dr} + i(2a\omega \sin^2 \theta - m) \frac{d\tilde{\varphi}}{dr} w_{nn} \right), \quad (\text{A15})$$

$$\begin{aligned} f_2 = & -\frac{1}{\omega^2} \left[\left(\frac{d^2 w_{nn}}{dr^2} - 2im \frac{d\tilde{\varphi}}{dr} \frac{dw_{nn}}{dr} - im \frac{d^2 \tilde{\varphi}}{dr^2} w_{nn} - m^2 \left(\frac{d\tilde{\varphi}}{dr} \right)^2 w_{nn} \right) \right. \\ & + 2ia\omega \sin^2 \theta \left(\frac{dw_{nn}}{dr} \frac{d\tilde{\varphi}}{dr} + w_{nn} \frac{d^2 \tilde{\varphi}}{dr^2} - im \left(\frac{d\tilde{\varphi}}{dr} \right)^2 w_{nn} \right) \\ & \left. - a^2 \omega^2 \sin^4 \theta \left(\frac{d\tilde{\varphi}}{dr} \right)^2 w_{nn} \right], \quad (\text{A16}) \end{aligned}$$

$$g_0 = \frac{i}{\omega} \rho w_{\bar{m}n}^{(1)} w_{\bar{m}n}^{(2)}, \quad (\text{A17})$$

$$g_1 = \frac{i}{\omega} w_{\bar{m}n}^{(1)} \left[-w_{\bar{m}n}^{(3)} + w_{\bar{m}n}^{(2)} \frac{d\rho}{dr} + 2\rho \frac{dw_{\bar{m}n}^{(2)}}{dr} - i(m - a\omega \sin^2 \theta) \rho w_{\bar{m}n}^{(2)} \frac{d\tilde{\varphi}}{dr} \right], \quad (\text{A18})$$

$$\begin{aligned} g_2 = & -\frac{i}{\omega} w_{\bar{m}n}^{(1)} \left[\frac{d}{dr} \left(w_{\bar{m}n}^{(3)} + \rho \frac{dw_{\bar{m}n}^{(2)}}{dr} \right) \right. \\ & \left. - i(m - a\omega \sin^2 \theta) \left(w_{\bar{m}n}^{(3)} - \rho \frac{dw_{\bar{m}n}^{(2)}}{dr} \right) \frac{d\tilde{\varphi}}{dr} \right], \quad (\text{A19}) \end{aligned}$$

$$h_0 = -\frac{1}{2} \frac{r^2 \bar{\rho}^2}{|dr/d\tau|} {}_{-2}S_{lm}^{aw} (w_{\bar{m}n}^{(1)})^2, \quad (\text{A20})$$

$$h_1 = -\frac{1}{2} \frac{\rho \bar{\rho}^2}{|dr/d\tau|} {}_{-2}S_{lm}^{aw} (w_{\bar{m}n}^{(1)})^2 \left(\frac{d}{dr} \left(\frac{r^2}{\rho} \right) + \rho^{-4} \frac{d}{dr} (\rho^3 r^2) \right), \quad (\text{A21})$$

$$h_2 = -\frac{1}{2} \frac{\rho \bar{\rho}^2}{|dr/d\tau|} {}_{-2}S_{lm}^{aw} (w_{\bar{m}n}^{(1)})^2 \frac{d}{dr} \left(\rho^{-4} \frac{d}{dr} (\rho^3 r^2) \right) \quad (\text{A22})$$

with

$$\tilde{\varphi} = \varphi + \int^r \frac{a}{\Delta} dr, \quad (\text{A23})$$

$$\rho = \frac{1}{r - ia \cos \theta}, \quad (\text{A24})$$

$$w_{nn} = -\frac{\mu r^2}{2\rho \Sigma^2} \left| \frac{dr}{d\tau} \right| \mathcal{L}_1^\dagger [\rho^{-4} \mathcal{L}_2^\dagger ({}_{-2}S_{lm}^{aw} \rho^3)], \quad (\text{A25})$$

$$w_{\bar{m}n}^{(1)} = \sqrt{\Theta} + i \sin \theta (aE - \frac{L_z}{\sin^2 \theta}), \quad (\text{A26})$$

$$w_{\bar{m}n}^{(2)} = \frac{r^2 \bar{\rho}}{\rho^2} \mathcal{L}_2^\dagger (\rho \bar{\rho} {}_{-2}S_{lm}^{aw}), \quad (\text{A27})$$

$$w_{\bar{m}n}^{(3)} = \frac{1}{2} r^2 \rho \mathcal{L}_2^\dagger \left(\rho^3 {}_{-2}S_{lm}^{a\omega} \frac{d}{dr} (\bar{\rho}^2 \rho^{-4}) \right), \quad (\text{A28})$$

where an overbar denotes the complex conjugate. The operator \mathcal{L}_s^\dagger is defined by

$$\mathcal{L}_s^\dagger = \frac{\partial}{\partial \theta} + a\omega \sin \theta - \frac{m}{\sin \theta} + s \cot \theta. \quad (\text{A29})$$

REFERENCES

- [1] R. A. Hulse and J. H. Taylor, *Astrophys. J.* **195** (1975), L51.
- [2] J. H. Taylor and J. M. Weisberg, *Astrophys. J.* **253** (1982), 908; *ibid.* **345** (1989), 434.
- [3] A. Abramovici, W. E. Althouse, R. W. P. Drever, Y. Gürsel, S. Kawamura, F. J. Rabb, D. Shoemaker, L. Sievers, R. E. Spero, K. S. Throne, R. E. Vogt, R. Weiss, S. E. Whitcomb and M. E. Zucker, *Science* **256** (1992), 325.
- [4] C. Brans and R. H. Dicke, *Phys. Rev.* **124** (1961), 925.
- [5] R. D. Reasenberg, I. I. Shapiro, P. E. MacNeil, R. B. Goldstein, J. C. Breidenthal, J. P. Brenkle, D. L. Cain and T. M. Kaufman, *Astrophys. J.* **234** (1979), L219.
- [6] R. V. Wagoner, *Phys. Rev.* **D1** (1970), 3209.
- [7] D. M. Eardley, D. L. Lee and A. P. Lightman, *Phys. Rev.* **D8** (1973), 3308.
- [8] D. M. Eardley, *Astrophys. J.* **196** (1975), L59.
- [9] C. M. Will, *Astrophys. J.* **214** (1977), 826.
- [10] C. M. Will and H. W. Zaglauer, *Astrophys. J.* **346** (1989), 366.
- [11] C. M. Will, *Phys. Rev.* **D50** (1994), 6058.
- [12] M. Shibata, K. Nakao and K. Nakamura, *Phys. Rev.* **D50** (1994), 7304.
- [13] P. Anninos, R. H. Price, J. Pullin, E. Seidel and W-M. Suen, *Phys. Rev.* **D52** (1995), 4462. See also E. Seidel, in *Relativity and Scientific Computing*, eds. by F. W. Hehl, R. A. Puntigam and H. Ruder (Springer-Verlag, Berlin Heidelberg, 1996).
- [14] $G_N = 1$ means, in this paper, that we set the Newtonian gravitational constant to be unity. This fixes the unperturbed values of the BD scalar field as $\phi_0 = (4 + 2\omega_{BD})/(3 + 2\omega_{BD})$. Since $\omega_{BD} > 500$, we find that $1 \leq \phi_0 < 1.001$.
- [15] C. W. Misner, K. S. Thorne and J. A. Wheeler, *Gravitation* (Freeman, San Francisco, 1973).
- [16] C. M. Will, *Theory and Experiment in Gravitational Physics* (Revised Edition) (Cambridge Univ. Press, Cambridge, 1993)
- [17] A. Ohashi, H. Tagoshi, and M. Sasaki, *Prog. Theor. Phys.* **96** (1996), 713.
- [18] This metric perturbation $h_{\mu\nu}^{(E)}$ is the same as $\theta_{\mu\nu}$ in [16], which is used to study BD theory in a weak field limit.
- [19] M. Sasaki and T. Nakamura, *Phys. Lett.* **89A** (1982), 68. See also M. Sasaki and T. Nakamura, *Prog. Theor. Phys.* **67** (1982), 1788; T. Nakamura and M. Sasaki, *Phys. Lett.* **89A** (1981), 185.
- [20] S. A. Teukolsky, *Astrophys. J.* **185** (1973), 635.
- [21] Y. Kojima and T. Nakamura, *Phys. Lett.* **96A** (1983), 335. See also Y. Kojima and T. Nakamura, *Prog. Theor. Phys.* **71** (1984), 79.
- [22] We are now analyzing gravitational waves for generic motions of a test particle moving off equatorial plane to study the dependence of the eccentricity or the Carter constant of the orbit. It will be published elsewhere.
- [23] Y. Mino, M. Shibata and T. Tanaka, *Phys. Rev.* **D53** (1996), 622. This paper discussed gravitational waves by a spinning test particle, but also gave the latest results for a non-spinning particle as a reference.
- [24] L. E. Simone and C. M. Will, *Class. Quantum Grav.* **9** (1992), 963.
- [25] N. Andersson, *Proc. R. Soc. Lond.* **439** (1992), 47.
- [26] E. W. Leaver, *Proc. Roy. Soc. Lond.* **A402** (1985), 285.

- [27] T. Nakamura and M. Sasaki, Phys. Lett. **106B** (1981), 69.
- [28] S. L. Shapiro and I. Wasserman, Astrophys. J. **260** (1982), 838.
- [29] M. P. Haugan, S. L. Shapiro and I. Wasserman, Astrophys. J. **257** (1982), 283.
- [30] T. Harada, T. Chiba, K. Nakao and T. Nakamura, Phys. Rev. **D55** (1997, to be published).
- [31] M. Shibata, Prog. Theor. Phys. **90** (1993), 595.

Figure Captions

Fig. 1: Waveforms of TGWs by a test particle with constant azimuthal angle θ falling into a Kerr black hole. We show two modes (h_+ and h_\times) of TGWs for $\theta = \pi/6$ ((a), (b)), $= \pi/3$ ((c), (d)) and h_+ mode for $\theta = \pi/2$ ((e)) (h_\times vanishes.). We choose a Kerr parameter $a=0$ (solid line), 0.5 (dashed line), 0.9 (dash-dotted line) and 0.99 (dotted line).

Fig. 2: Emitted energy of TGWs shown in Fig. 1. Circle (filled), square, triangle and circle (open) represents the cases of $a = 0$, $a = 0.5$, $a = 0.9$ and $a = 0.99$, respectively.

Fig. 3: Waveforms of SGWs by a test particle with constant azimuthal angle θ falling into a Kerr black hole for $\omega_{BD} = 500$. We show SGWs for $\theta = \pi/6$ ((a)), $= \pi/3$ ((b)) and $= \pi/2$ ((c)). We choose a Kerr parameter $a=0$ (solid line), 0.5 (dashed line) and 0.9 (dash-dotted line). We find that they do not depend very much on the azimuthal angle and the Kerr parameter, although we find a phase difference depends on a .

Fig. 4: Energy spectrum of SGWs shown in Fig. 3. Solid, dashed, dash-dotted and dotted lines represent $a = 0$, $a = 0.5$, $a = 0.9$ and $a = 0.99$, respectively. We find that the frequencies which emits largest energy spectrum corresponds to that of the QNM. All lines (solid line ($a = 0$), dashed one ($a = 0.5$), dash-dotted one ($a = 0.9$) and dotted one ($a = 0.99$)) almost coincide with each other.

Fig. 5: Emitted energy of SGWs shown in Fig. 3. Circle (filled), square, triangle and circle (open) represent $a = 0$, $a = 0.5$, $a = 0.9$ and $a = 0.99$, respectively. They also do not depend very much on the azimuthal angle.

Fig. 6: The tail part of the SGW is fitted by one of the QNMs, which corresponds to the largest peak in the energy spectrum (Fig. 4). Solid line represents the SGW, while dashed line denotes the waveform fitted by one of the QNMs ((a) $a = 0$, (b) $a = 0.5$ and (c) $a = 0.9$).

Fig. 7: Emitted energy by a non-spherical dust shell collapsing into a Schwarzschild black hole ((a) prolate shell and (b) oblate shell) for $\omega_{BD} = 500$. A spherically symmetric shell does not generate TGWs, while SGWs are emitted. Since the $l = 0$ mode dominates in the SGW, the emitted energy of the SGW does not depend on a deformation parameter δ . The SGW dominates the TGWs for $\delta_1(= -0.07) < \delta < \delta_2(= 0.07)$.

Fig. 8: Emitted energy by non-spherical dust shell collapsing into a Kerr black hole ((a) prolate shell and (b) oblate shell) for $\omega_{BD} = 500$. Dashed, dash-dotted and dotted lines represent $a = 0.5$, $a = 0.9$ and $a = 0.99$ respectively. Since the system is no longer spherically symmetric for any values of δ , we expect the TGWs as well as the SGW. At δ_0 , which is not zero and depends on a rotation parameter a ($\delta_0 \sim 0.02, 0.08$ and 0.10 for $a = 0.5, 0.9$ and 0.99 , respectively), the emitted energy of TGW takes a minimum value. As a increases, its minimum energy and the corresponding deformation parameter δ_0 increase. Since the $l = 0$ mode dominates in the SGW, the emitted energy of SGW does not depend on a deformation parameter δ . It also depends little on a . Both energies of TGW and SGW decrease for $\delta \gtrsim \delta_{cr}^{(TGW)}$ and $\delta \gtrsim \delta_{cr}^{(SGW)}$ because of a phase cancellation effect. The SGW dominates the TGWs for $\delta_1(= -0.05, 0.03$ and 0.05 for $a = 0.5, 0.9$ and 0.99) $< \delta < \delta_2(= 0.09, 0.11$ and 0.12 for $a = 0.5, 0.9$ and 0.99).

TABLES

Binary System	Coma cluster ($\sim 80\text{Mpc}$)	Virgo cluster ($\sim 20\text{Mpc}$)	Our Galaxy ($\sim 10\text{kpc}$)
NS-NS, BH-BH	$\omega_{BD} \lesssim 60$	$\lesssim 250$	$\lesssim 5 \times 10^5$
NS-BH	$\omega_{BD} \lesssim 400$	$\lesssim 1,700$	$\lesssim 3.5 \times 10^6$

Table 1: The upper bound of the BD coupling constant ω_{BD} if the SGW with a polarization information independently of the TGW is detected.

Fig. 1 (a)

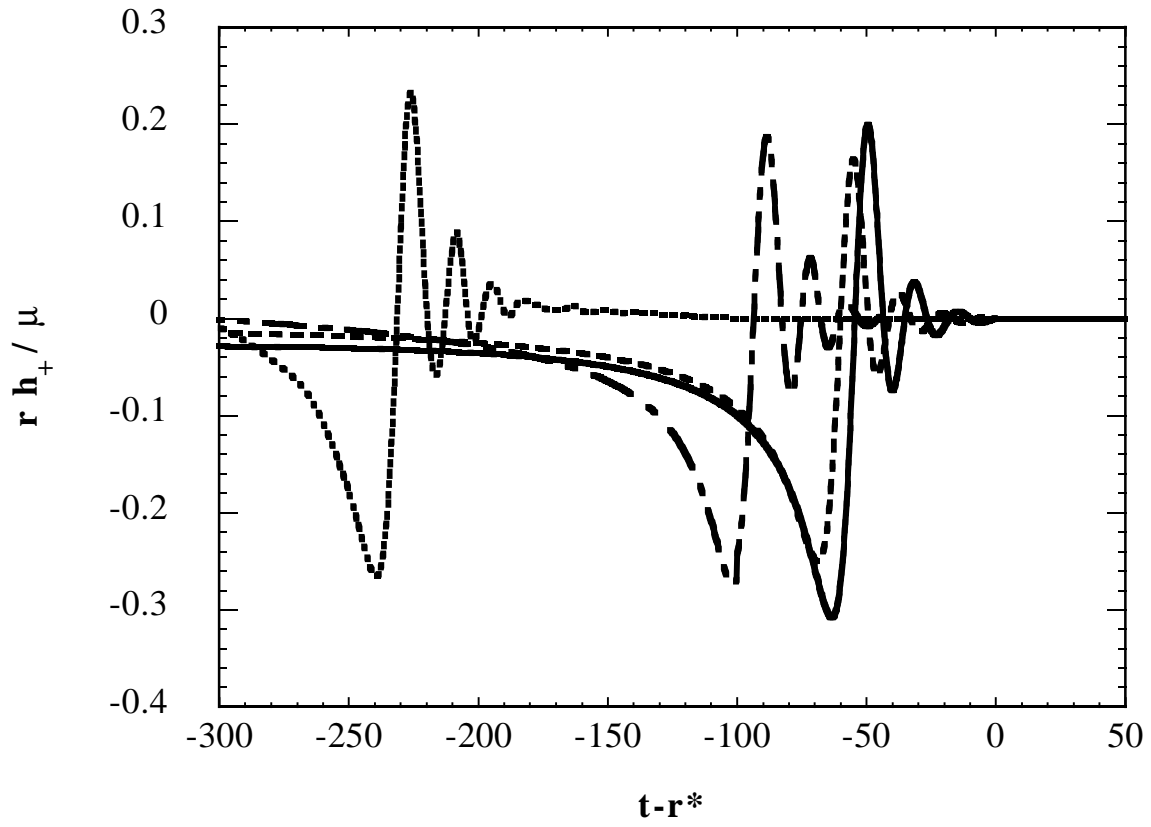


Fig. 1 (b)

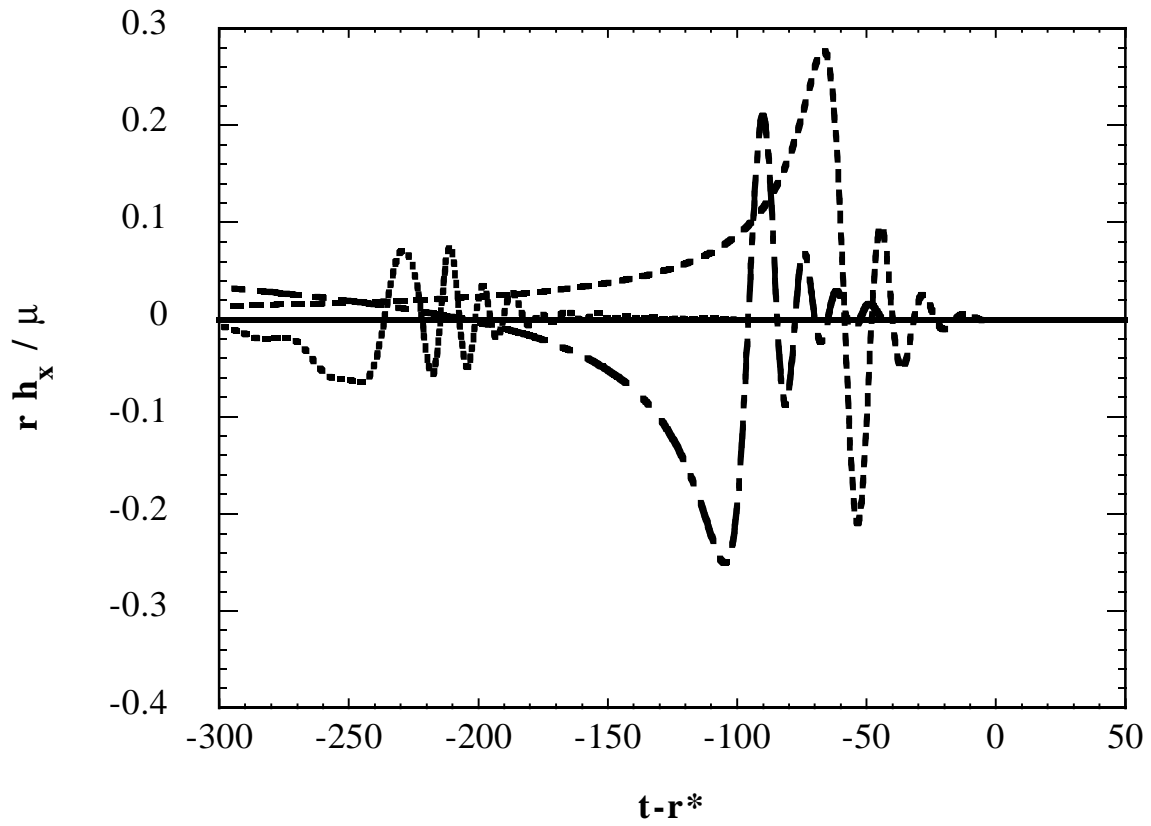


Fig. 1 (c)

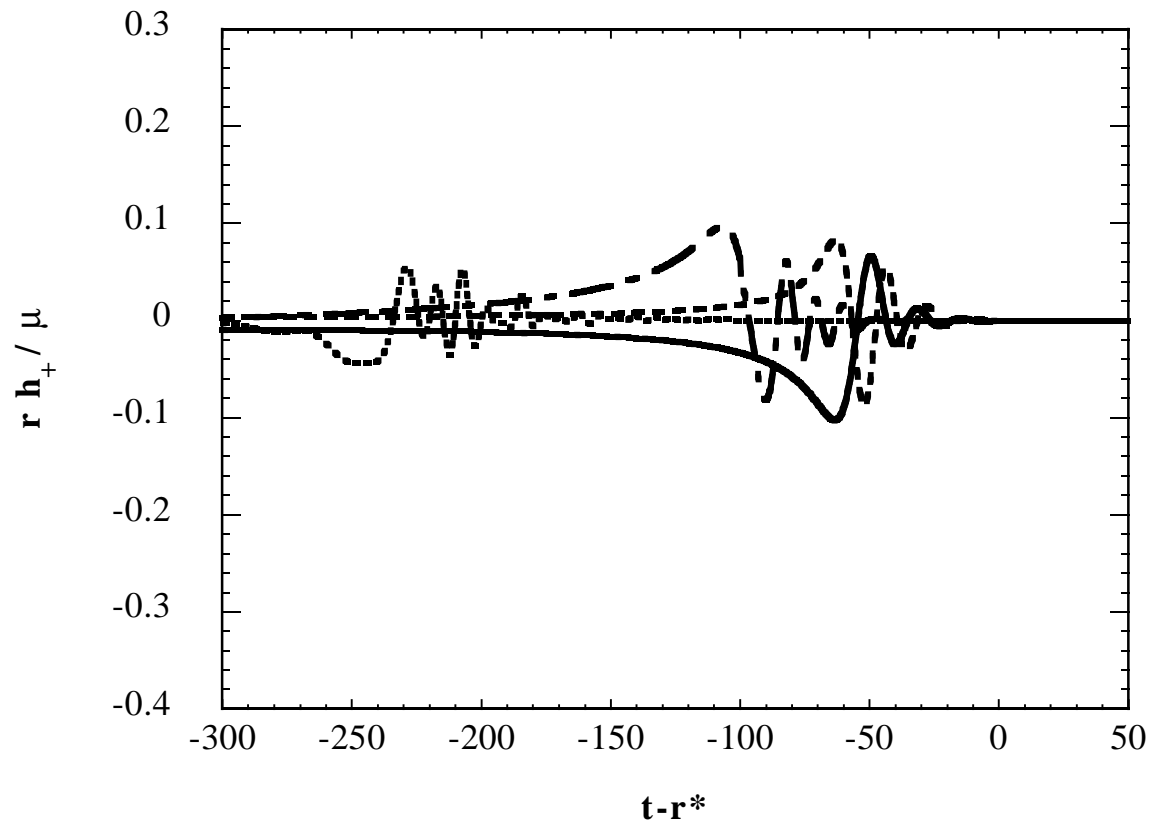


Fig. 1 (d)

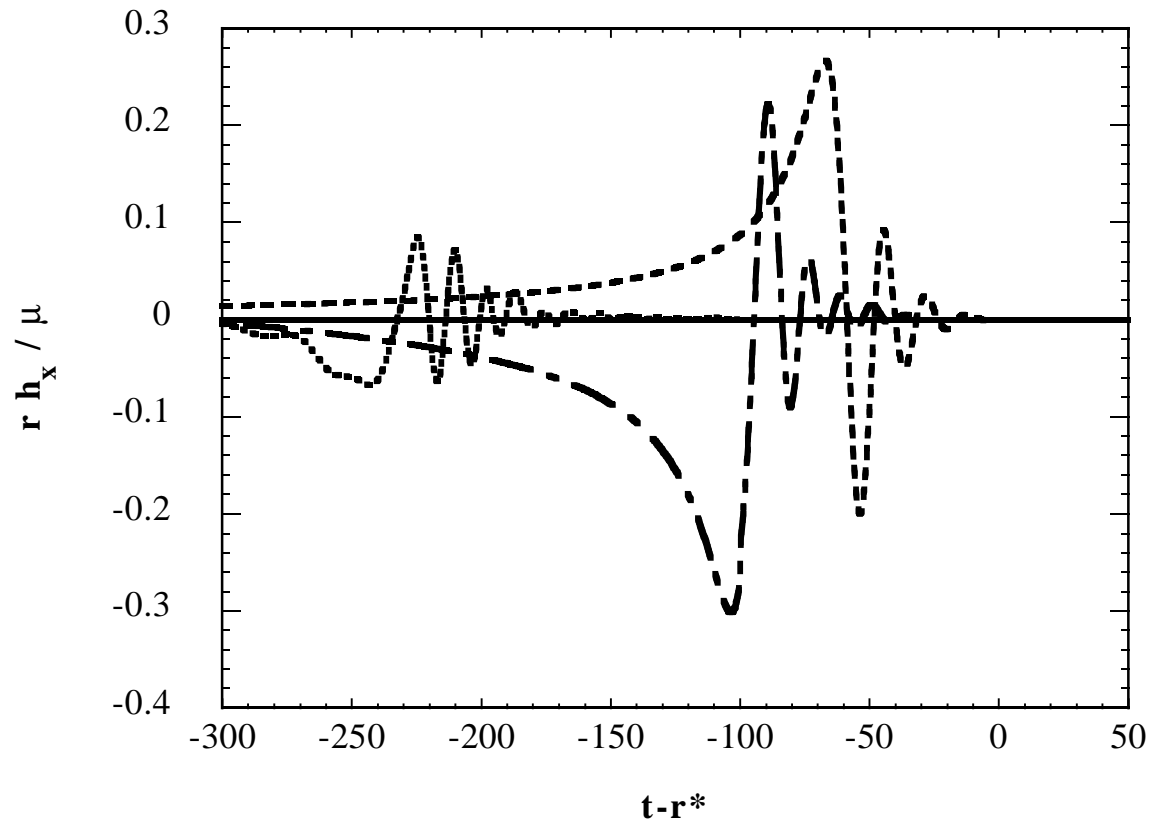


Fig. 1 (e)

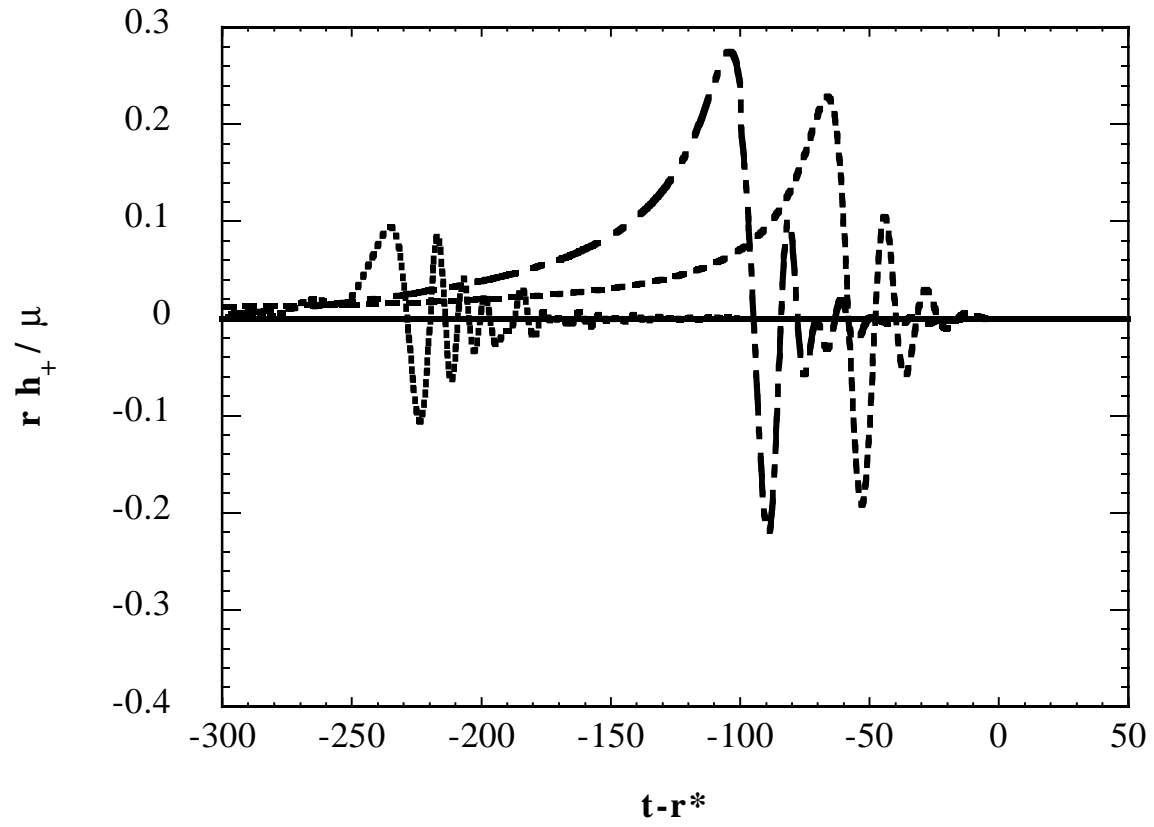


Fig. 2

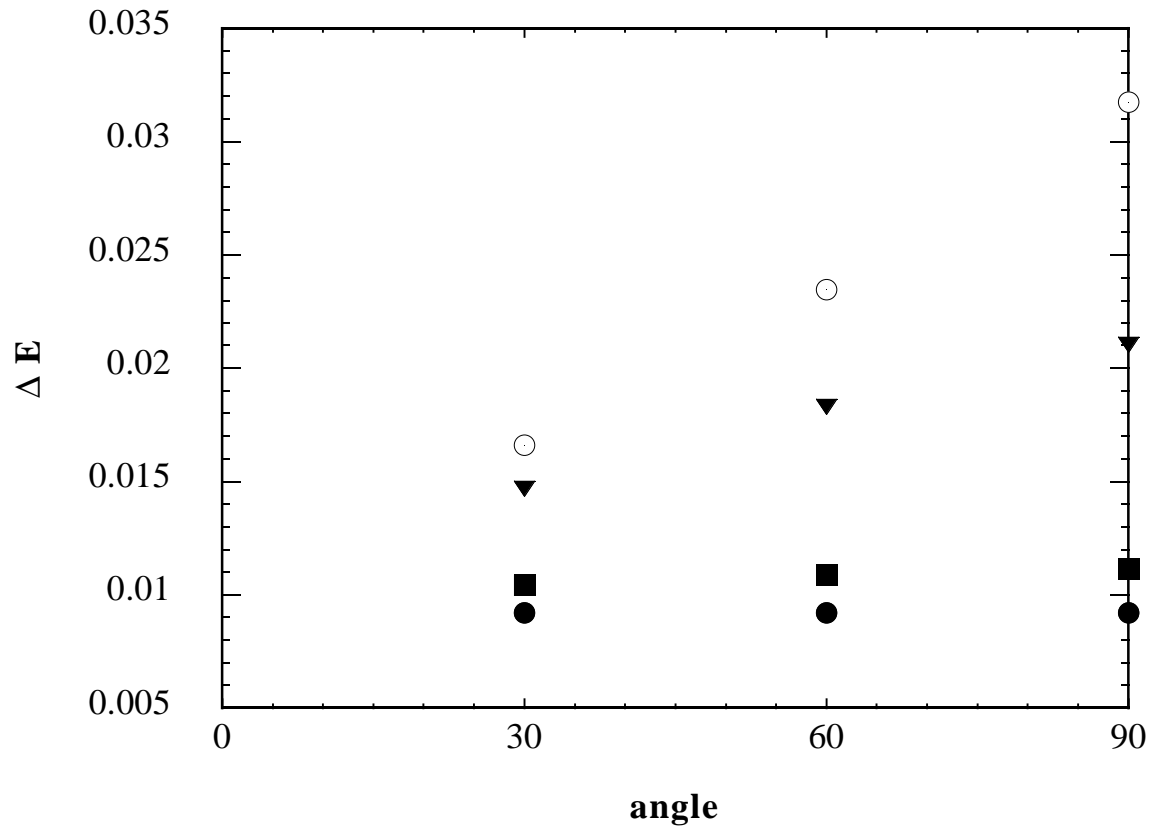


Fig. 3 (a)

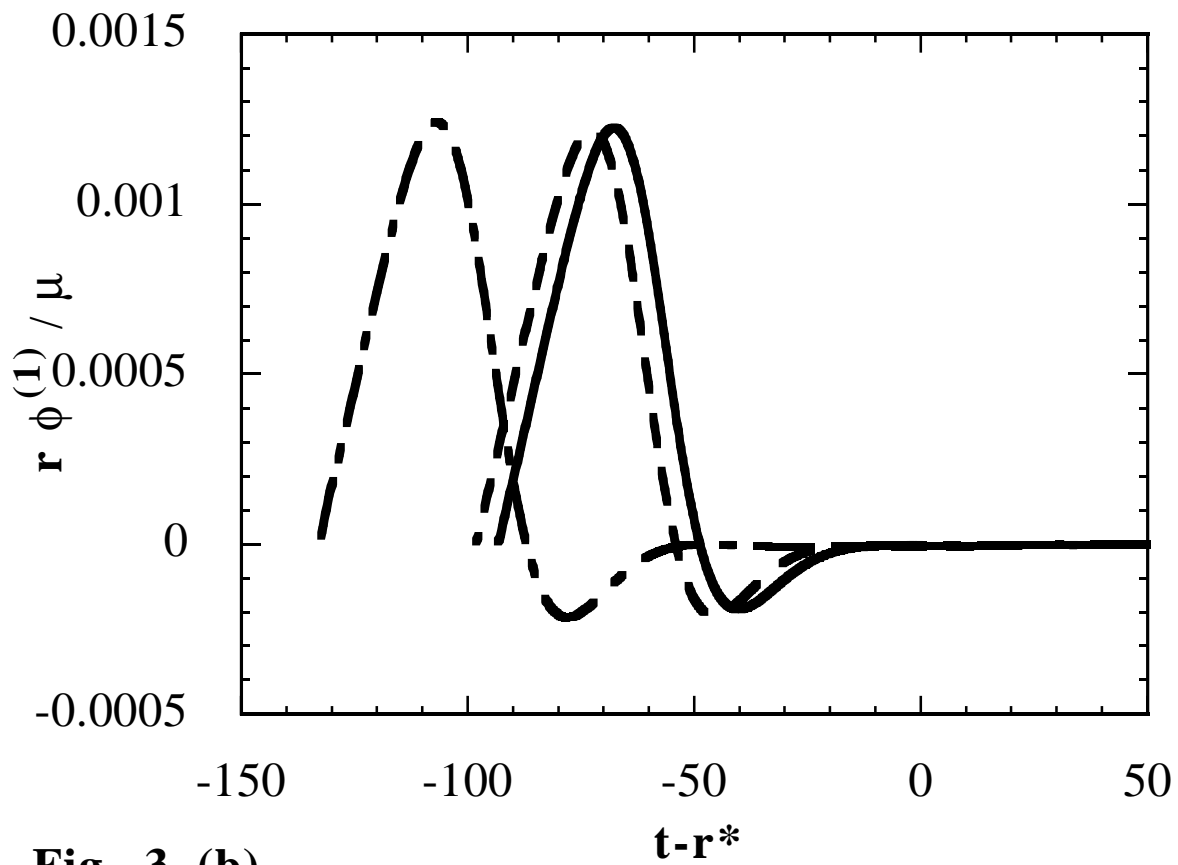


Fig. 3 (b)

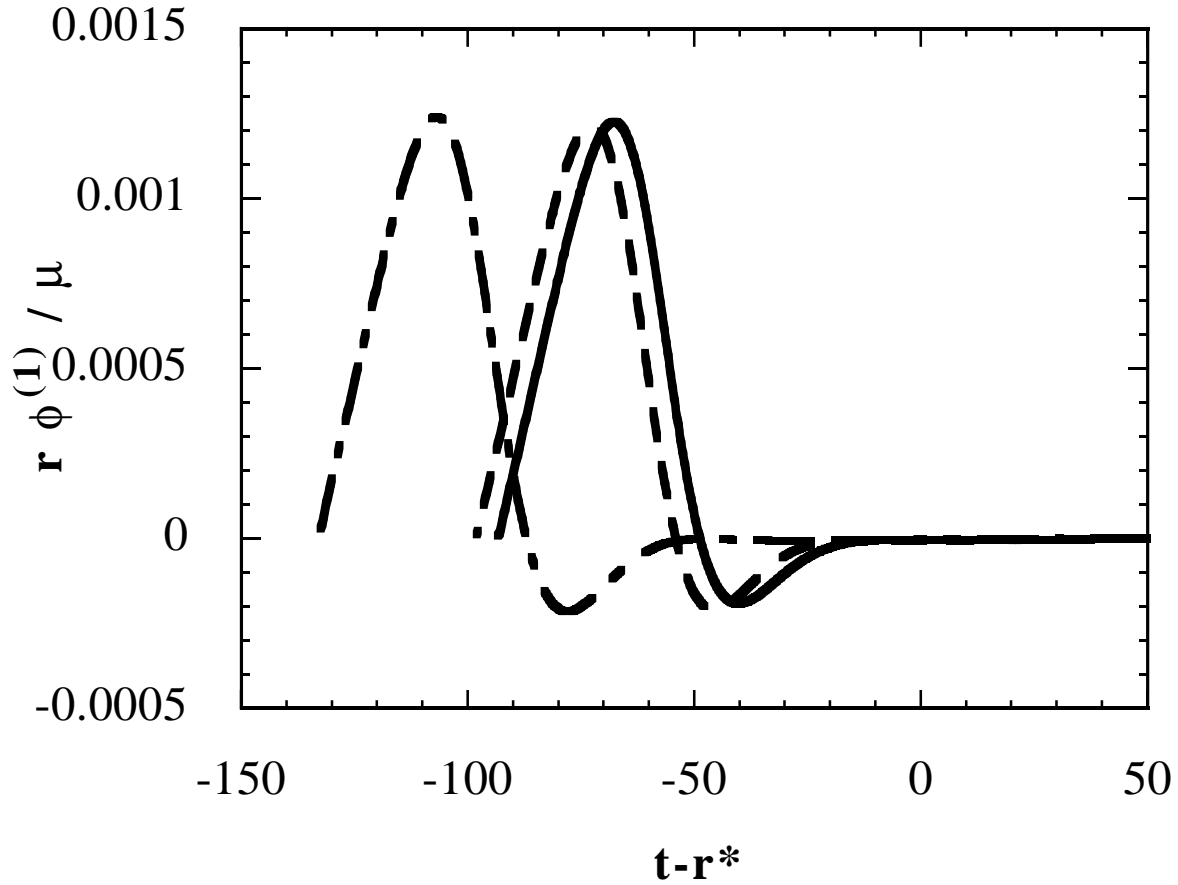


Fig. 3 (c)

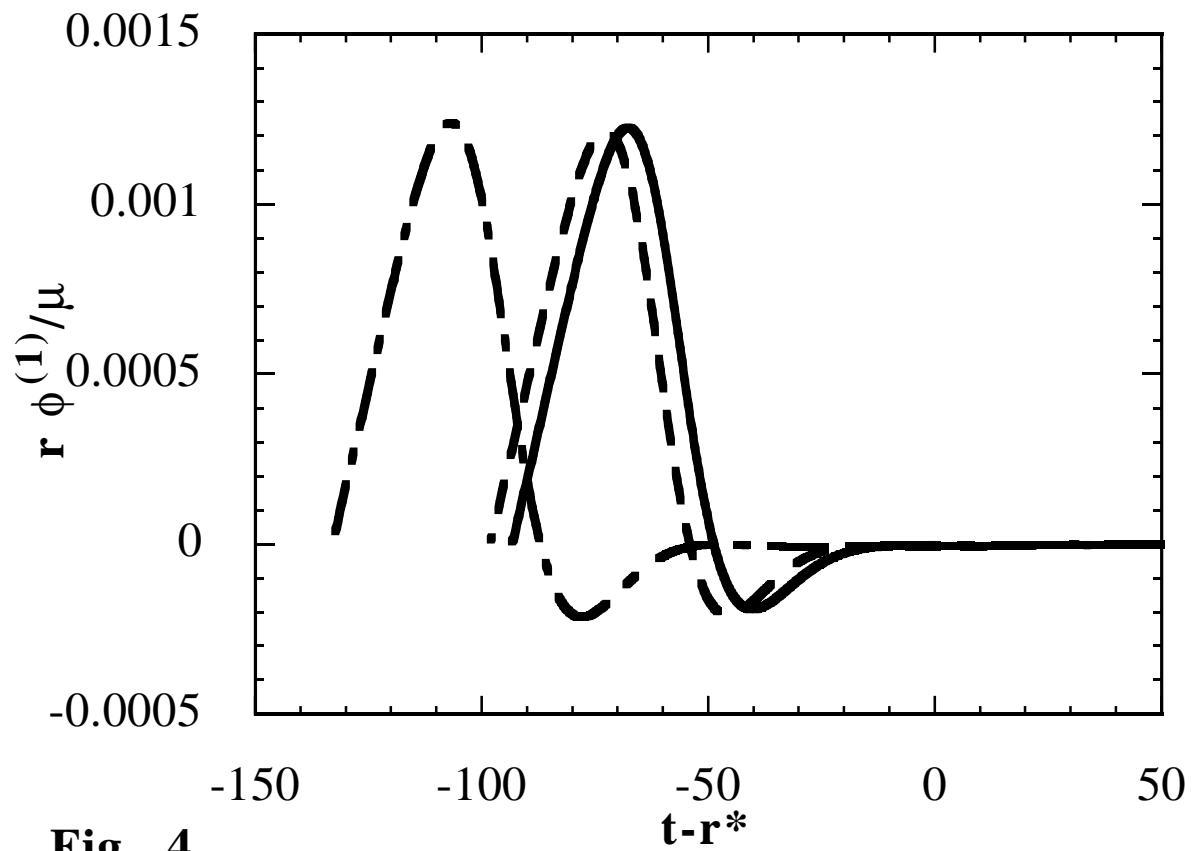


Fig. 4

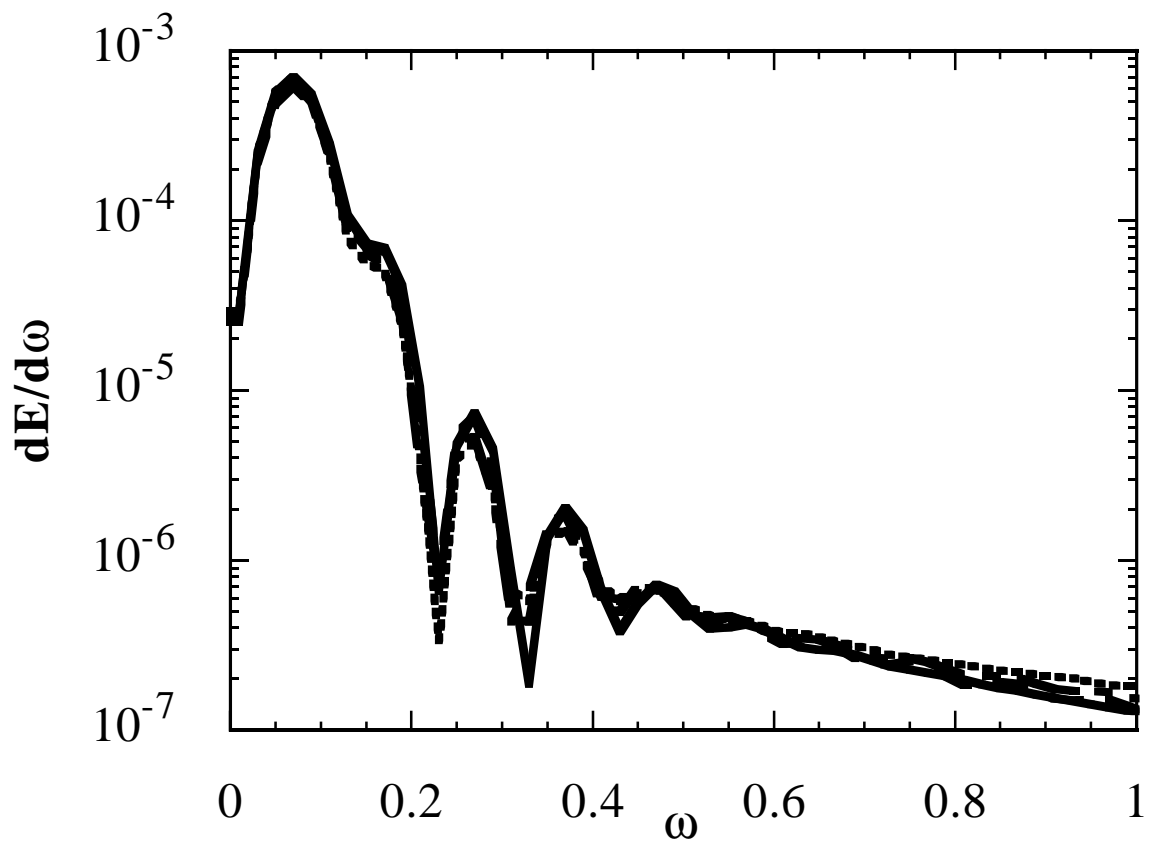


Fig. 5

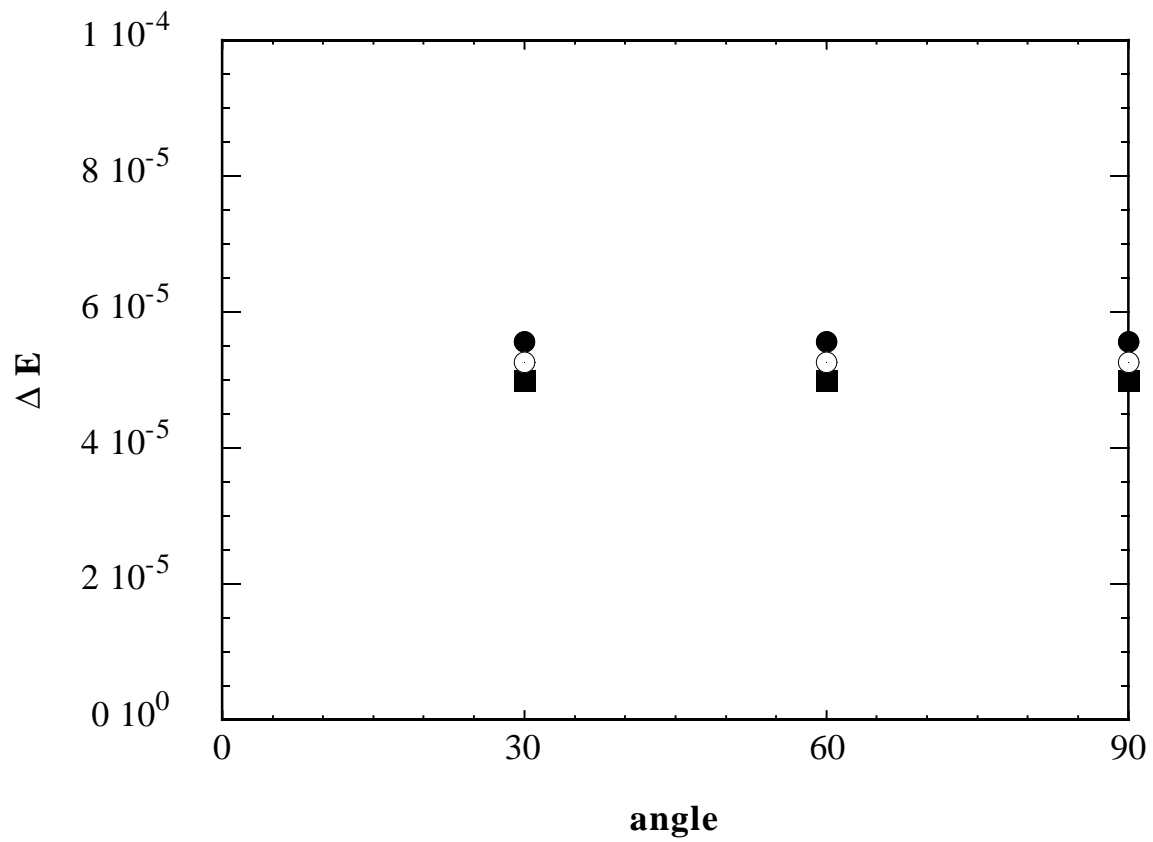


Fig. 6 (a)

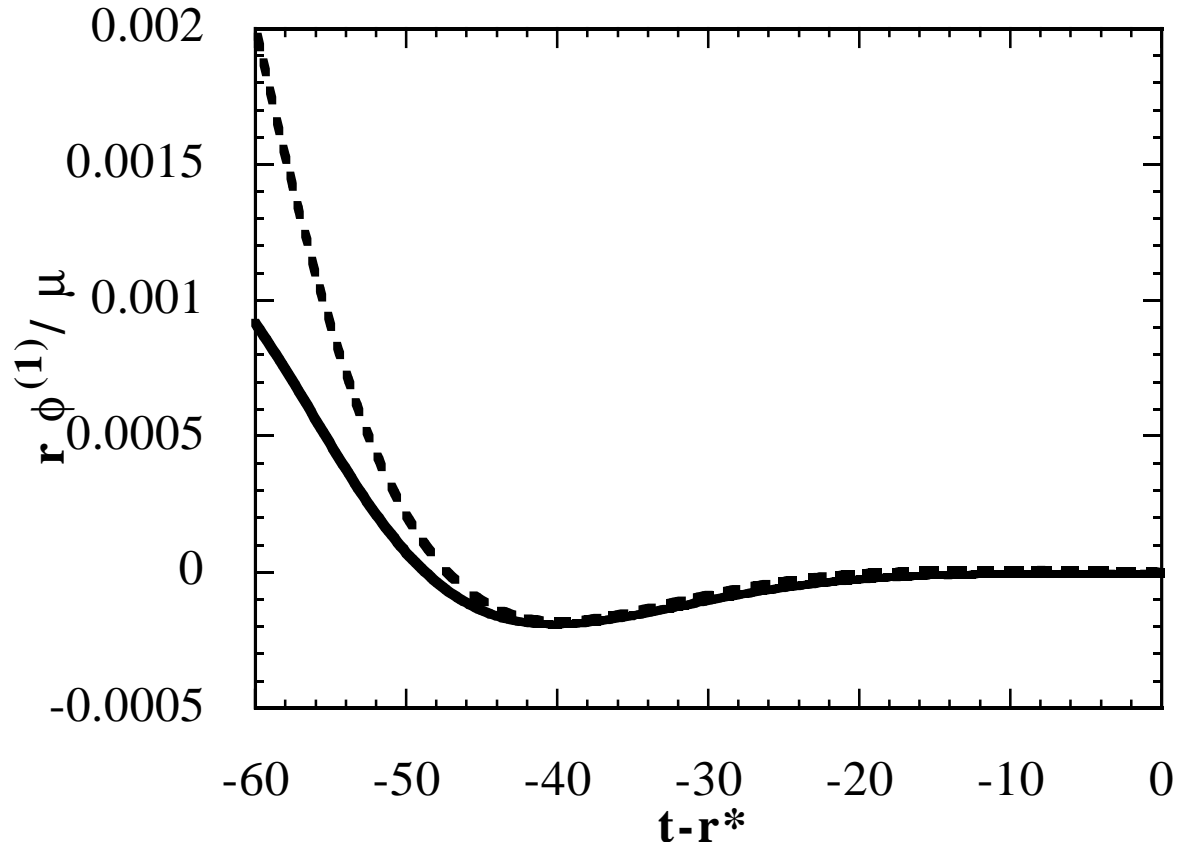


Fig. 6 (b)

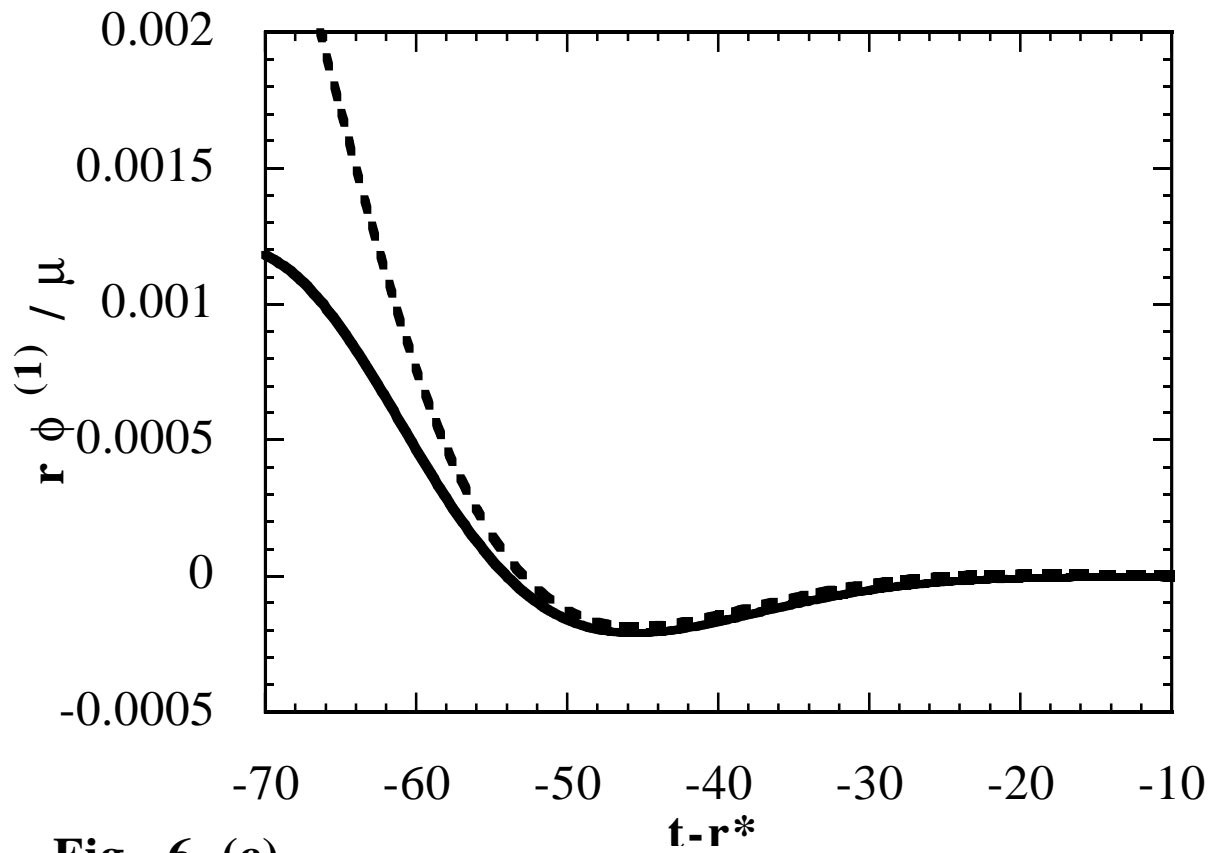


Fig. 6 (c)

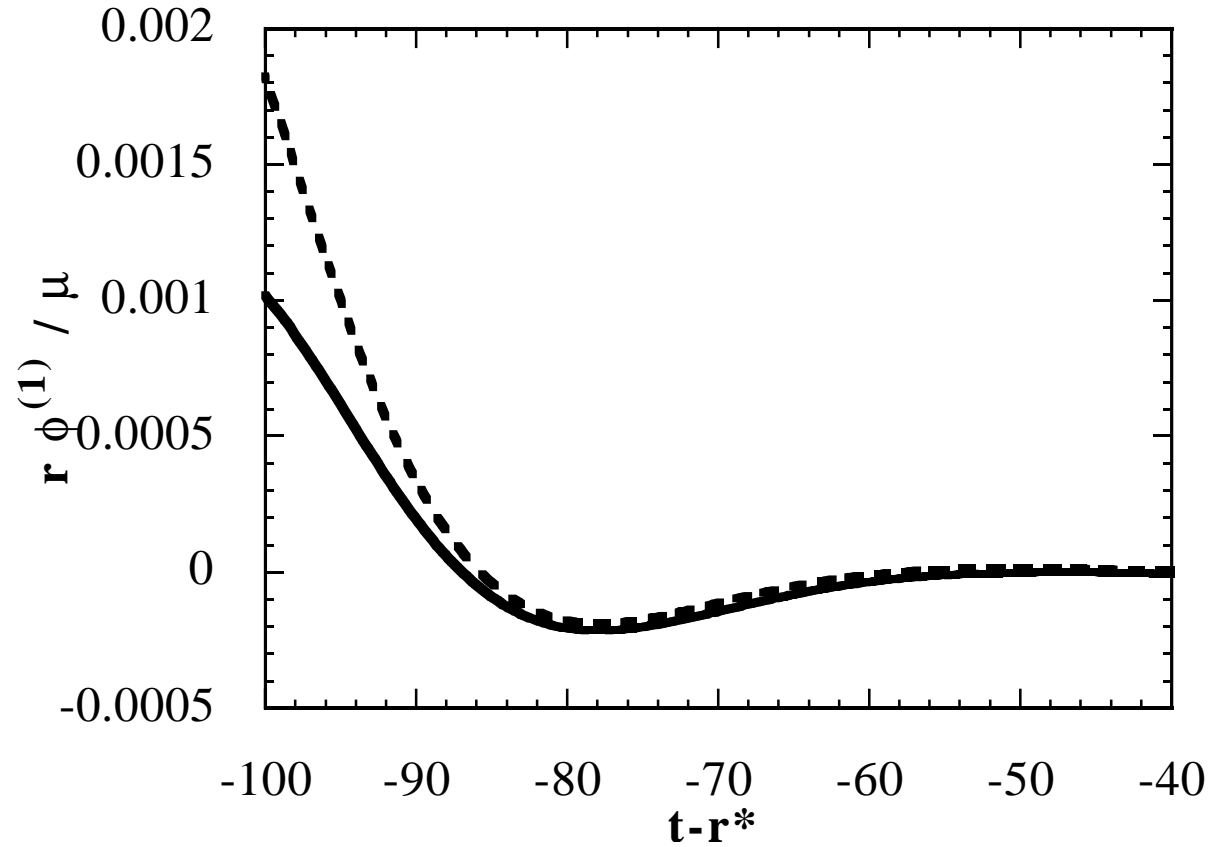


Fig. 7 (a)

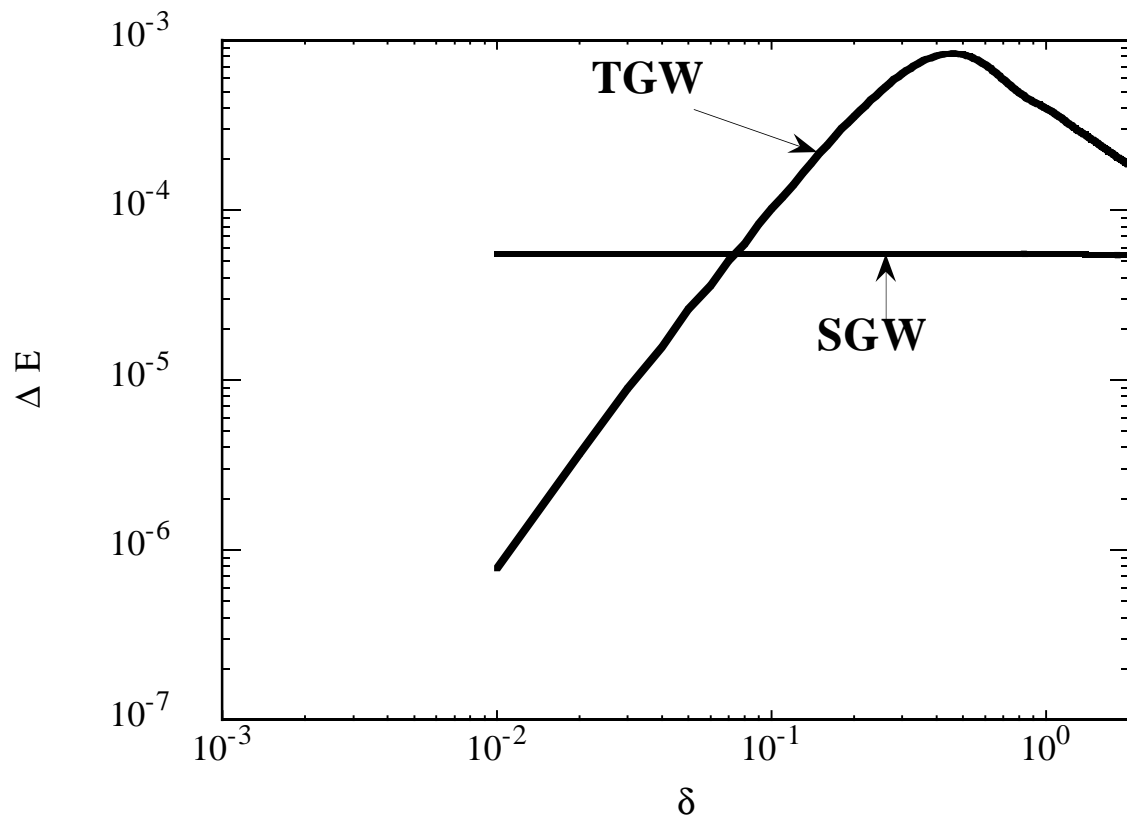


Fig. 7 (b)

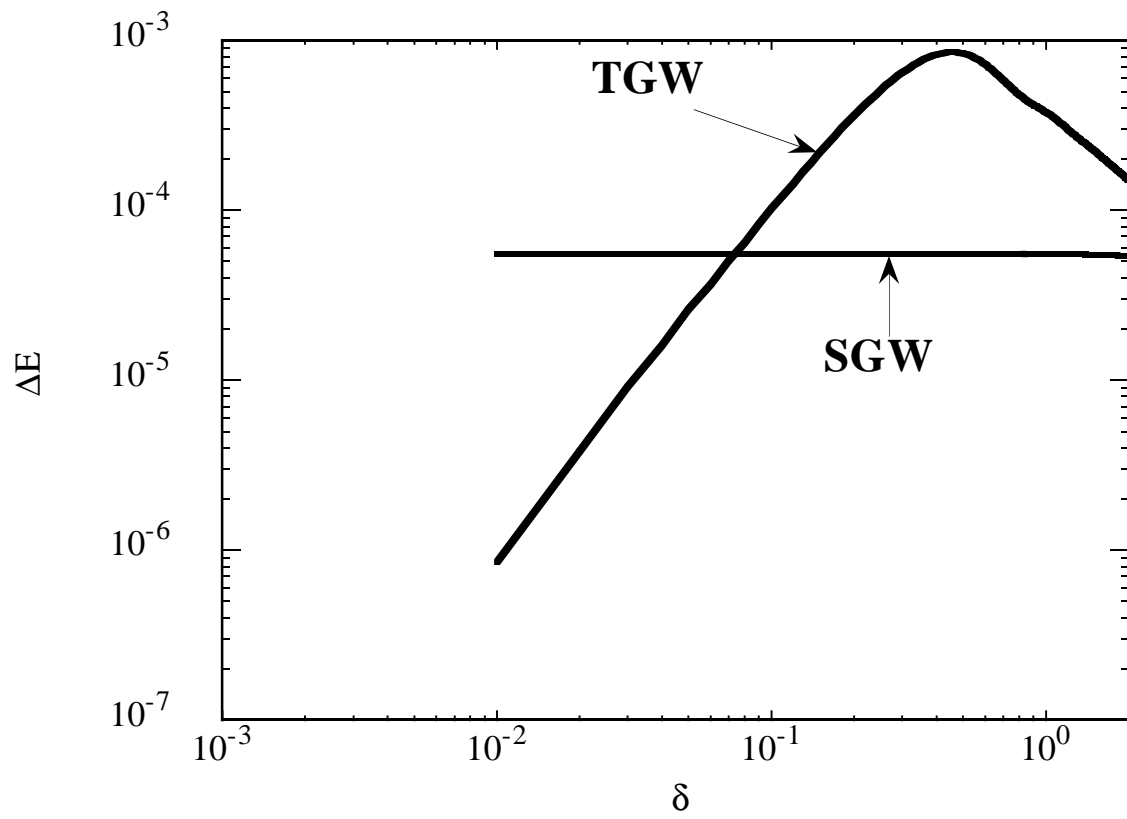


Fig. 8 (a)

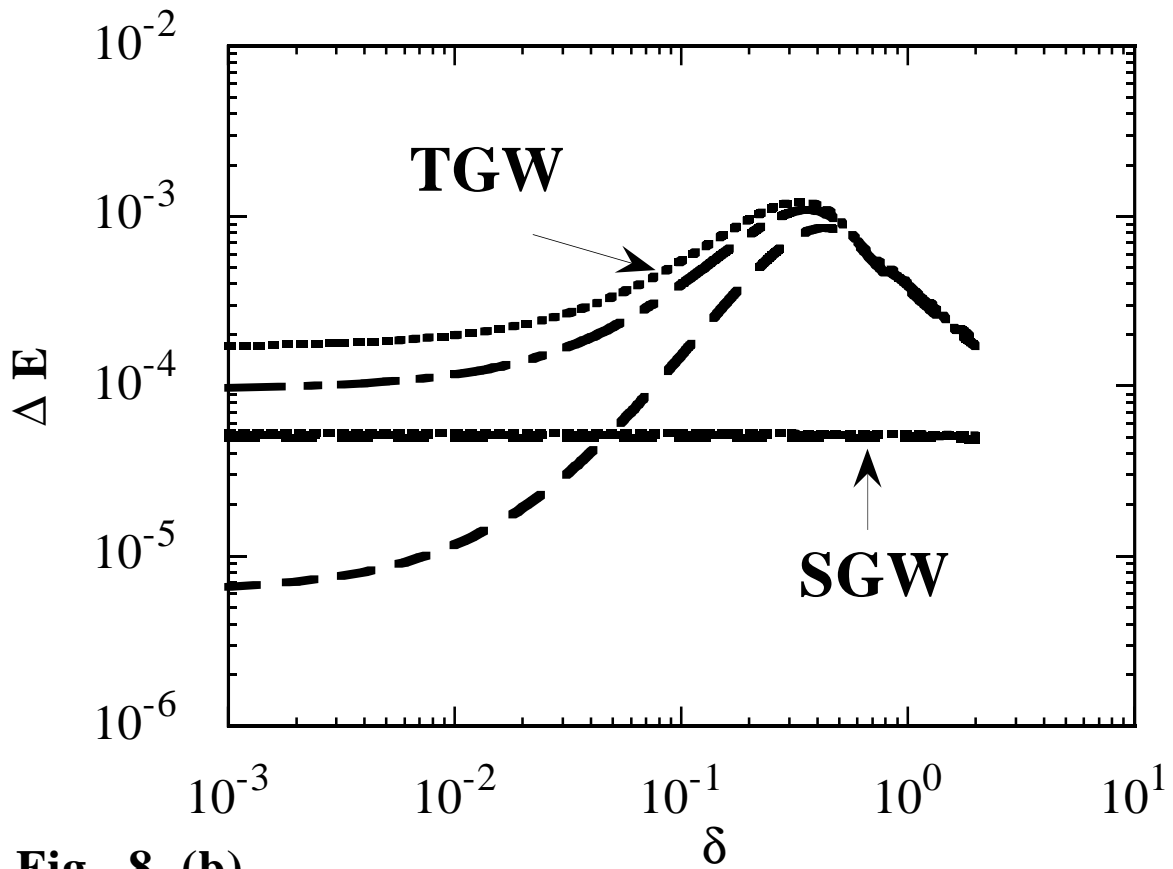


Fig. 8 (b)

